20131301OA (3/3)

厚生労働科学研究費補助金

第３次対がん総合戦略研究事業

がん化学予防剤の開発に関する基礎及び臨床研究

平成２５年度　総括・分担研究報告書

（３／３）

研究代表者

武藤　倫弘　（国立がん研究センター研究所）

研究分担者

田中　卓二　（岐阜大学）
塚本　徹哉　（藤田保健衛生大学）
高山　哲治　（徳島大学）
石川　秀樹　（京都府立医科大学）
鈴木　貞夫　（名古屋市立大学）
今井　俊夫　（国立がん研究センター研究所）
岩崎　　基　（国立がん研究センター
がん予防・検診研究センター）
鰐渕　英機　（大阪市立大学）
清水　雅仁　（岐阜大学）
高橋　　智　（名古屋市立大学）
窪田　直人　（東京大学）

平成２６（２０１４）年５月

High susceptibility of heterozygous (+/*fa*) lean Zucker rats to 7,12-dimethylbenz(*a*)anthracene-induced mammary carcinogenesis

TOSHIO IMAI[1,2], YOUNG-MAN CHO[1], MAMI TAKAHASHI[2], TSUKASA KITAHASHI[2], SHIGEAKI TAKAMI[1], AKIYOSHI NISHIKAWA[1] and KUMIKO OGAWA[1]

[1]Division of Pathology, National Institute of Health Sciences, Setagaya-ku, Tokyo 158-8501; [2]Central Animal Division, National Cancer Center Research Institute, Chuo-ku, Tokyo 104-0045, Japan

Received December 11, 2012; Accepted January 22, 2013

DOI: 10.3892/or.2013.2326

Abstract. Susceptibility to 7,12-dimethylbenz(*a*)anthracene (DMBA)-induced mammary carcinogenesis was investigated in lean Zucker *(+/fa)* rats carrying one mutated leptin receptor gene and wild-type controls (+/+). Rats with both genotypes were given a single DMBA administration and divided into two groups, one group was fed on basal diet mixed with 10% corn oil and the other was fed on basal diet alone. The minimum latency period of palpable carcinomas in +/*fa* rats of both groups was 8 weeks following DMBA treatment, in contrast to the 11-12 weeks in +/+. The incidence and multiplicity of carcinomas increased or showed a tendency for increase in the early stages in +/*fa* rats of both groups as compared to the +/+ counterparts. The volumes of carcinomas showed a tendency to increase in the corn oil diet groups of both genotypes. The major histopathological phenotype of carcinomas in all groups was well-differentiated without distinct atypia (multiplicity, 0.69-1.09/rat), but moderately/poorly differentiated carcinomas with atypia were also found, predominantly in +/*fa* rats (0.09-0.21). These latter tumors were characterized by elevated ERK activity but not estrogen receptor expression. Serum leptin concentrations in +/*fa* rats at 7 weeks of age were higher than those in +/+ and were elevated by the corn oil diet; however, no obvious change was detected in other serum parameters examined. In conclusion, +/*fa* rats proved more susceptible to DMBA-induced mammary carcinogenesis than +/+ controls, and hyperleptinemia was suggested to contribute to tumor growth as well as to susceptibility to tumorigenesis and more aggressive phenotypes in Zucker lean rats.

Correspondence to: Dr Toshio Imai, Central Animal Division, National Cancer Center Research Institute, 5-1-1 Tsukiji, Chuo-ku, Tokyo 104-0045, Japan
E-mail: toimai@ncc.go.jp

Key words: mammary, carcinoma, leptin, 7,12-dimethylbenz(*a*)-anthracene, Zucker rat

Introduction

A relationship between obesity and breast cancer risk has been proposed based on epidemiological data, a positive association with increasing body mass index being found particularly in postmenopausal women (1-4). Although the underlying mechanisms have yet to be fully clarified, increased concentrations of circulating sex hormones are likely to contribute at least in part (5). In addition, circulating levels of an adipokine leptin, which is secreted mainly from adipose tissue and limits food intake and increases energy expenditure (6), was recently suggested to have a role independent of obesity indices in breast tumorigenesis (7). In estrogen receptor (ER)-positive breast cancer cells, leptin has been demonstrated to stimulate aromatase expression and cell proliferation, and both in ER-positive and -negative breast cancer cells, leptin induced transactivation of ErbB tyrosine kinase receptors, such as the epidermal growth factor receptor (EGFR) and ErbB-2 (HER2/Neu), resulting in the induction of cell proliferation and increased survival (8-10).

To investigate the effects of obesity on mammary carcinogenesis, a number of animal models, featuring inherited obesity or feeding of a high fat/calorie diet, were employed. Fatty Zucker (*fa/fa*) rats, which have autosomal recessive mutation in the leptin receptor gene (11), develop hyperinsulinemia, but blood glucose remains at normal levels (12). In addition, they demonstrate significantly increased serum triglyceride, total cholesterol and leptin levels (12,13). Lean Zucker (+/*fa* and +/+) rats, by contrast, exhibit normal appearing metabolic functions and have been utilized as controls in chemically-induced mammary carcinogenesis investigations (14-17). In a previous study, the latency period and/or the incidence of mammary carcinomas were reported to be shorter and greater, respectively, in female *fa/fa* than +/*fa* and +/+ rats treated with 7,12-dimethylbenz(*a*)anthracene (DMBA) (15,17). However, in another study, female Zucker (*fa/fa*) rats treated with *N*-methyl-*N*-nitrosourea (MNU) showed a lower incidence of mammary carcinomas compared to lean Zucker controls (+/*fa* and +/+) (14). A number of factors may contribute to the discrepancy between the DMBA- and MNU-treated rats, and it remains unclear which obesity-associated internal parameters, such as hyperin-

sulinemia, hyperleptinemia or hyperlipidemia, fundamentally affect mammary carcinogenesis.

We recently compared serum biochemical parameters between lean Zucker (+/*fa*) and (+/+) rats in combination with or without an obesity-inducing 10% corn oil diet, to clarify whether lean Zucker (+/*fa*) rats might also be more sensitive to the high fat diet than the +/+ controls (18). Serum leptin concentrations were higher in the (+/*fa*) case at 7 weeks of age (~140 pg/ml as compared to ~80 pg/ml in +/+; $P<0.01$), although the difference was significantly smaller at 12 weeks of age, and serum concentrations of other parameters including insulin, triglycerides and total cholesterol were similar between the two genotypes. In addition, both +/*fa* and +/+ rats fed basal diet mixed with 10% corn oil showed higher serum leptin levels than those fed basal diet alone, but no other parameters examined were altered by the obesity-inducing diet.

In the present study, to clarify the effects of hereditary and dietary hyperleptinemia on mammary carcinogenesis, lean Zucker (+/*fa*) rats with and without 10% corn oil feeding were utilized in a DMBA-induced mammary carcinogenesis model along with control lean Zucker (+/+) rats. In the present study, latency period and growth rates of mammary carcinomas were assessed by regular palpation, and at the termination, histopathological, immunohistochemical and western blot analyses were performed to determine expression profiles of estrogen- and intracellular signaling cascade-related proteins in the mammary carcinomas, as well as serum biochemistry for obesity-associated parameters. The data demonstrated +/*fa* rats to indeed be more susceptible to DMBA-induced mammary carcinogenesis than +/+ controls, with hyperleptinemia appearing to be partly associated with tumor growth as well as with susceptibility to tumorigenesis and a more aggressive phenotype in an estrogen-independent manner.

Materials and methods

Chemicals and animals. DMBA was purchased from Sigma Chemical (St. Louis, MO, USA) and dissolved in sesame oil at 10 mg/ml prior to administration. A total of 100 female Zucker rats (lean phenotype) at 5 weeks of age were purchased from Charles River Japan (Kanagawa, Japan) and acclimated for 1 week prior to genotyping by the method of Phillips *et al* (19). Throughout the acclimatization and experimental periods, the animals were housed at a maximum of 3 or 4 per plastic cage with white wood chips (Sankyo Laboratory Service, Tokyo, Japan) for bedding and transferred to clean cages with fresh bedding twice a week in a standard air-conditioned animal room (24±1°C, 55±5% relative humidity, 12 h light and dark cycle). All animals had free access to basal diet (CRF-1; Oriental Yeast Co., Tokyo, Japan) and tap water until the start of the experiment.

Experimental protocol. Sixty-six +/*fa* and 32 +/+ rats at 7 weeks of age received an intragastric administration of DMBA (50 mg/kg body weight) by gavage, and the animals of each genotype were then divided into basal diet (CRF-1; 357 kcal/100 g) and 10% corn oil diet (CRF-1-based, Oriental Yeast; 414 kcal/100 g) groups. The present dose level of DMBA at 50 mg/kg body weight was selected based on our previous experiments, in which palpable mammary tumors were induced at adequate incidences for detection of endogenous and exogenous tumor promoting and/or inhibitory factors in Sprague-Dawley (20) and F344 rats (21). The dietary concentration of corn oil at 10% was selected based on the previously reported effective concentrations of linoleic acid for promotion of rat mammary tumor development (22). General conditions and mortality were checked daily and body weight was measured once a week during the experimental period. The amounts of supplied and residual diet were weighted weekly in order to calculate the average daily food intake per week. Following DMBA administration, a veterinary scientist (T.I.) palpated cervix, thorax and abdomen of awake rats to detect mammary tumors once weekly. The length, width and height of each tumor were measured using a caliper and tumor volumes were calculated as follows: Volume = (length) x (width) x (height) x $\pi/6$.

For endpoints for this study, the rats were sacrificed when demonstrating over 20% decrease in body weight excluding total tumor weight and/or when symptoms of poor physical condition, such as decrease in locomotor activity, were found. Volume of mammary tumors was not considered important in this regard, since change in tumor volume was a key item for evaluation of the effects of rat genotype and corn oil diet. All remaining rats were sacrificed at 32 weeks following DMBA administration. The present study design was approved by the Animal Care and Utilization Committee of the National Institute of Health Sciences.

Necropsy and histopathology. At the end of the experimental period, blood samples were collected from the abdominal aorta of all surviving animals under ether anesthesia. Serum was separated and maintained at -80°C until use. Following euthanasia by exsanguination under ether anesthesia, animals were subjected to necropsy. Whole skins with mammary glands and tumors were removed, and the sizes of all mammary tumors were recorded. Tumor volumes were calculated in the same manner as for palpable tumors. Sections of frozen tissue of randomly selected mammary tumors of rats in all groups were prepared with liquid nitrogen and stored at -80°C until use. The remaining tumor and mammary tissues were fixed in 10% neutral buffered formalin, processed routinely to paraffin-embedded sections at 4-5 μm, and stained with hematoxylin and eosin (H&E) for histopathological analysis. Animals that died or that were sacrificed on becoming moribund were similarly necropsied and included for the sequential palpable tumor and postmortem analyses.

Immunohistochemistry. Primary antisera for the leptin receptor (goat polyclonal; Neuromics Antibodies, Edina, MN, USA; 1:1,000 dilution), smooth muscle actin (mouse clone 1A4; Dako, Glostrup, Denmark; 1:200), leptin (rabbit polyclonal; Santa Cruz Biotechnology, Santa Cruz, CA, USA; 1:200), ER α (mouse clone 6F11; Novocastra, Newcastle, UK; 1:50 or 1:500), ER β (rabbit polyclonal; Affinity BioReagents, Rockford, IL, USA; 1:100) and aromatase (rabbit polyclonal; Abcam, Cambridge, MA, USA; 1:500), were utilized for immunohistochemistry. Analyzed mammary tumors were selected from all groups, on the basis of the genotype, diet and phenotypes. Paraffin sections 5, 5, 10 and 10 carcinomas from the +/+-basal diet, +/+-corn oil diet, +/*fa*-basal diet and

+/*fa*-corn oil diet groups, respectively, were used for leptin receptor, leptin, smooth muscle actin and ER α, and frozen sections of 3, 4, 4 and 5 each were for ER β and aromatase. Antigen retrieval for paraffin sections was carried out in an autoclave for 10 min at 121˚C in 10 mM citrate buffer (pH 6.0) for leptin receptor, smooth muscle actin and ER α. The streptavidin-biotin-peroxidase complex method (StreptABComplex/HRP; Dako) was used to determine the expression and localization of each antigen, and sections were lightly counterstained with hematoxylin for microscopic examination. Negative controls without primary antibody reactions were set for each antigen using serial sections. The positivities for ER α in over 1,000 mammary adenocarcinoma cells were assessed on each paraffin section to give percentage values.

Western blot analysis. Twelve mammary tumors and four normal mammary tissue samples of the +/+-basal diet, +/+-corn oil diet and +/*fa*-basal diet groups were homogenized in extraction buffer (50 mM Tris-HCl pH 7.4, 3 mM EDTA, 100 mM NaCl, 1% Tween-20, 10 mM sodium orthovanadate, 1 mM PMSF, 10 μg/ml leupeptin, 20 μg/ml aprotinin) and centrifuged at 14,000 g for 20 min. Equal amounts of protein samples (50 μg) from collected supernatants were subjected to SDS-polyacrylamide gel electrophoresis (SDS-PAGE) on 5-20% gradient acrylamide gels (ATTO, Tokyo, Japan), and the separated proteins were transferred to polyvinylidene difluoride membranes (Whatman, Sanford, ME, USA). Immunoblotting was performed using rabbit polyclonal antibodies against ER β (Affinity BioReagents), aromatase (Abcam), signal transducer and activator of transcription (STAT)3 and phospho-STAT3 (Thy705) (Cell Signaling Technology, Danvers, MA, USA), extracellular signal-regulated kinase (ERK)1/2 and phospho-ERK1/2 (R&D Systems, Minneapolis, MN, USA) or monoclonal antibodies against β-actin (mouse clone AC-15; Sigma), followed by exposure to peroxidase-labeled anti-rabbit or mouse polyclonal goat antibodies (Dako) and development of signals with TMB 3,3',5,5' tetramethylbenzidine (ATTO). Semi-quantitative analyses were performed using Scion Image (alpha4.0.3.0; Scion, Frederick, MD, USA).

Serum biochemistry. Concentrations of serum leptin, adiponectin, insulin and insulin-like growth factor (IGF)-I were determined for randomly selected almost half and one third of samples from +/+- and +/*fa*-groups, respectively, using rat/mouse enzyme immunoassay kits from Yanaihara Institute (Shizuoka, Japan), Adipogen (Incheon, Korea), Mercodia (Uppsala, Sweden) and R&D Systems, respectively. Other serum biochemical parameters including triglyceride, total cholesterol and glucose were measured for all samples except for those lost due to sampling error at SRL (Tokyo, Japan).

Statistical analysis. The survival rates and incidence of palpable or histopathologically defined mammary tumors were analyzed for inter-group differences by the Fisher's exact probability test. Data for body weights and multiplicity, volume and latency of mammary tumors, ER α-positivity in mammary adenocarcinoma sections, serum biochemistry and western blot analysis data were examined with the Student's or the Welch's t-test following the F-test. Significance was inferred at the 5, 1 and 0.1% levels.

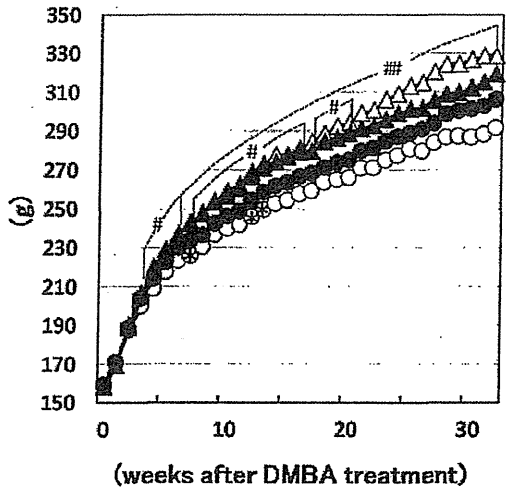

Figure 1. Body weight curves. Open circles, +/+-basal diet; open triangles, +/+-10% corn oil diet; closed circles, +/*fa*-basal diet; closed triangles, +/*fa*-10% corn oil diet. *P<0.05 vs. +/+-basal diet (difference with the genotype basis); #P<0.05, ##P<0.01 vs. +/+-basal diet or +/*fa*-basal diet (difference with the diet basis).

Results

Survival rates, body weights and food intake. At the end of the experiment, survival rates were 94% (15/16), 81% (13/16), 85% (28/33) and 85% (28/33) in the +/+-basal diet, +/+-corn oil diet, +/*fa*-basal diet and +/*fa*-corn oil diet groups, respectively, with no significant variation among the groups. Body weight curves of each group are shown in Fig. 1. Values of the +/+-corn oil diet group were higher than those of the +/+-basal diet group from week 4 to the end of the experiment. In addition, the body weights of the +/*fa*-corn oil diet group were higher than those of the +/*fa*-basal diet group from week 8 to 20. The differences between +/+ and +/*fa* of both the basal and the corn oil diet groups were markedly smaller than those between the basal diet and corn oil diet groups in each genotype. Average food intake of the +/+-basal diet, +/+-corn oil diet, +/*fa*-basal diet and +/*fa*-corn oil diet groups were 11.8-14.2, 9.2-12.8, 11.4-14.3 and 9.7-12.6 g/rat/day, respectively, and those of the corn oil groups showed a tendency for decrease as compared to those of the basal diet groups in both genotypes.

Sequential changes in palpable mammary carcinomas. The minimum latency periods of palpable mammary carcinomas, which were histopathologically defined postmortem, were 8 weeks following DMBA administration in both the +/*fa*-basal and +/*fa*-corn oil diet groups, considerably shorter than the 11-12 weeks in the +/+-basal and +/+-corn oil diet groups (Fig. 2A). Incidence and multiplicity of palpable mammary carcinomas were increased or showed a tendency for increase in the early stages in +/*fa*-basal and +/*fa*-corn oil diet groups as compared to their +/+-counterparts, whereas their volume showed a tendency for increase in the corn oil diet groups of both +/+ and +/*fa* as compared to the basal diet groups (Fig. 2B and C).

Table I. Final incidence and multiplicity data for mammary tumors.

	+/+ genotype				+/*fa* genotype			
	Basal diet (n=16)		Corn oil diet (n=16)		Basal diet (n=33)		Corn oil diet (33)	
	Incidence (%)	Multiplicity (No./rat)	Incidence (%)	Multiplicity (No./rat)	Incidence (%)	Multiplicity (No./rat)	Incidence (%)	Multiplicity (No./rat)
Carcinoma	7 (44)	0.88±1.41[a]	8 (50)	0.69±0.79	20 (61)	1.30±1.49	19 (58)	0.94±1.27
Adenoma	1 (6)	0.06±0.25	1 (6)	0.06±0.25	0	-	1 (3)	0.03±0.17
Fibroadenoma	4 (25)	0.25±0.45	3 (19)	0.25±0.58	7 (21)	0.30±0.64	5 (15)	0.24±0.61
Fibroma	0	-	0	-	2 (6)	0.06±0.24	0	-

[a]Means ± SDs.

Table II. Final volumes of mammary tumors.

	+/+ genotype				+/*fa* genotype			
	Basal diet (n=16)		Corn oil diet (n=16)		Basal diet (n=33)		Corn oil diet (n=33)	
	No. of tumors	Volume (cm^3/tumor)	No. of tumors	Volume (cm^3/tumor)	No. of tumors	Volume (cm^3/tumor)	No. of tumors	Volume (cm^3/tumor)
Carcinoma	14	2.06±4.14	11	6.72±8.89	43	2.92±6.29	31	6.86±12.14
Adenoma	1	0.01	1	0.21	0	-	1	0.11
Fibroadenoma	4	0.26±0.23	4	18.80±31.95	10	1.49±2.54	8	4.97±13.34
Fibroma	0	-	0	-	2	35.56±50.21	0	-

Values are means ± SDs.

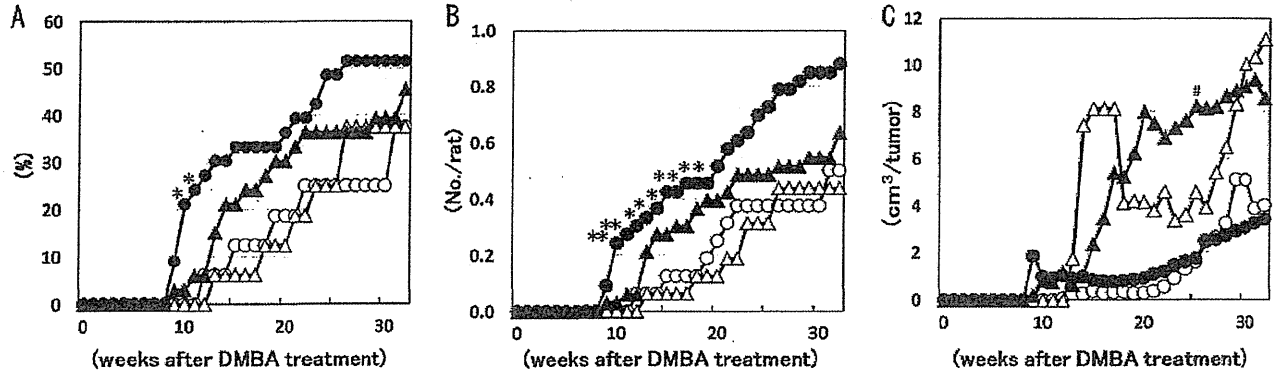

Figure 2. Sequential changes in palpable mammary carcinomas. (A) Cumulative incidence of rats with carcinomas; (B) cumulative mean number of carcinomas per rat (multiplicity); (C) cumulative mean volume of nodule/mass of carcinomas. Open circles, +/+-basal diet; open triangles, +/+-10% corn oil diet; closed circles, +/*fa*-basal diet; closed triangles, +/*fa*-10% corn oil diet. *P<0.05, **P<0.01 vs. +/+-basal diet (difference with the genotype basis); #P<0.05 vs. +/*fa*-basal diet (difference with the diet basis).

Final incidence, multiplicity and volume of mammary tumors. Incidence, multiplicity and volume findings for histopathologically defined mammary tumors are summarized in Table I. Histopathologically, mammary tumors could be classified as adenocarcinomas and benign lesions, such as adenomas, fibroadenomas and fibromas. Incidence and multiplicity of mammary carcinomas showed a tendency for increase (~1.5-fold) in the +/*fa*-basal diet group as compared with +/+-controls, but no influence on the genotype was noted in the corn oil diet groups. Furthermore, the corn oil diet showed no apparent effect on the incidence and multiplicity of mammary carcinomas in each genotype. Incidence and multi-

Table III. Distribution of sub-classified mammary carcinomas based on the morphological phenotypes among the groups.

	+/+ genotype				+/*fa* genotype			
	Basal diet (n=16)		Corn oil diet (n=16)		Basal diet (n=33)		Corn oil diet (n=33)	
	Incidence (%)	Multiplicity (No./rat)	Incidence (%)	Multiplicity (No./rat)	Incidence (%)	Multiplicity (No./rat)	Incidence (%)	Multiplicity (No./rat)
Moderately/poorly differentiated carcinoma with atypia	1 (6)	0.06±0.25[a]	0	-	6 (18)	0.21±0.48	3 (9)	0.09±0.29
Well-differentiated carcinoma without distinct atypia	7 (44)	0.81±1.22	8 (50)	0.69±0.79	16 (48)	1.09±1.49	17 (52)	0.85±1.28

[a]Means ± SDs.

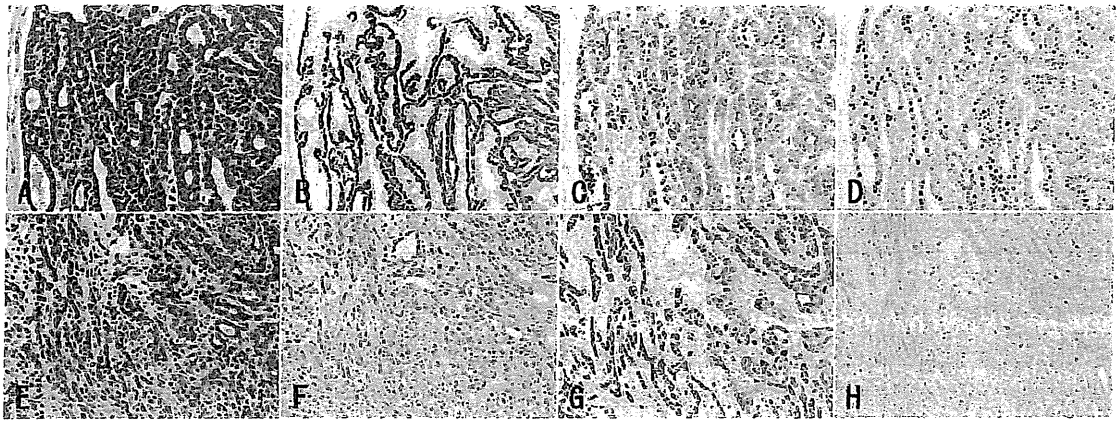

Figure 3. Histopathology and immunohistochemistry of mammary carcinomas. (A-D) A well differentiated carcinoma without distinct atypia in a +/+ rat fed basal diet; (E-H) a moderately/poorly differentiated carcinoma with atypia in a +/*fa* rat fed basal diet. (A and E) H&E. Immunohistochemistry for (B and F) α smooth muscle actin, showing cytoplasmic positivity for myoepithelial cells; (C and G) leptin receptor membranous positivity in carcinoma cells; (D and H) estrogen receptor α nuclear positivity in carcinoma cells. Original magnification, x360.

plicity of adenomas, fibroadenomas and fibromas were similar among the groups. On the other hand, volume of mammary carcinomas as well as fibroadenomas showed a tendency for increase by the corn oil diet with both +/+ and +/*fa* genotypes (Table II).

Histopathology, immunohistochemistry and western blot analysis of mammary carcinomas. Mammary adenocarcinomas found in the present experiment were mainly well differentiated without distinct nuclear atypia; however, some carcinomas showed moderately/poorly differentiated phenotypes with nuclear atypia (Fig. 3A and E). Well differentiated carcinomas showed papillotubular structures with cribriform patterns, and the tubules were generally well demarcated with α smooth muscle actin-positive myoepithelial cells (Fig. 3B). On the other hand, moderately/poorly differentiated carcinomas showed distinct invasion with small cord/glandular or scattering patterns mainly in the peripheral portion, and interstitial cell proliferation was prominent (Fig. 3F). The distribution of the sub-classified mammary carcinomas based on the morphological phenotypes among the groups is summarized in Table III. Incidence and multiplicity of moderately/poorly differentiated carcinomas with atypia showed a tendency for increase in the +/*fa*-basal diet and+/*fa*-corn oil diet groups as compared with their +/+-counterparts (Table III). The latency period of moderately/poorly differentiated carcinomas with atypia was shorter than that of well differentiated carcinomas without distinct atypia in the +/*fa*-basal diet group (Fig. 4).

To clarify expression profiles of leptin- and estrogen-related proteins in the well differentiated carcinomas without distinct atypia and moderately/poorly differentiated carcinomas with atypia, immunohistochemical and immunoblot analyses were performed. Mammary carcinomas of both phenotypes showed various expression intensities for leptin receptors (Fig. 3C and G) and leptin (data not shown), whereas the cases with atypia showed lower ER α-positivities than those without distinct atypia in the +/*fa*-basal diet and +/*fa*-corn oil diet groups (Table IV, Fig. 3D and H). For ER

Table IV. Estrogen receptor (ER) α-positivity in sub-classified mammary carcinomas based on the morphological phenotypes.

	+/+ genotype				+/*fa* genotype			
	Basal diet		Corn oil diet		Basal diet		Corn oil diet	
	No. of carcinomas examined	ER α-positivity (%)	No. of carcinomas examined	ER α-positivity (%)	No. of carcinomas examined	ER α-positivity (%)	No. of carcinomas examined	ER α-positivity (%)
Moderately/poorly differentiated carcinoma with atypia	1	1.0	0	-	7	8.9±3.9[b]	3	14.1±11.2
Well-differentiated carcinoma without distinct atypia	5	28.2±16.6[a]	6	24.2±14.2	6	36.4±15.0	10	28.9±11.4

[a]Means ± SDs; [b]P<0.01 vs. well-differentiated carcinoma without distinct atypia.

Table V. Serum biochemistry data at terminal sacrifice.

	+/+ genotype				+/*fa* genotype			
	Basal diet		Corn oil diet		Basal diet		Corn oil diet	
	No. of samples	Serum levels	No. of samples	Serum levels	No. of samples	Serum levels	No. of samples	Serum levels
Triglycerides (mg/dl)	16	340.8±138.7	15	311.5±221.5	31	392.3±312.6	31	279.6±146.5
Total cholesterol (mg/dl)	16	119.7±22.9	15	108.3±25.4	31	125.0±38.5	31	105.7±17.5[b]
Glucose (mg/dl)	16	134.6±15.9	15	145.3±15.4	31	133.7±13.3	31	141.9±17.5[b]
Leptin (pg/ml)	8	314.4±96.4	7	691.9±540.1	13	191.6±123.1	12	506.4±439.3[b]
Adiponectin (μg/ml)	8	6.7±1.4	7	7.1±3.8	12	4.0±1.0[a]	12	6.5±1.4[c]
Insulin (ng/ml)	8	2.1±0.8	7	1.5±1.0	14	1.3±0.9	13	1.5±1.1
IGF-I (ng/ml)	8	612.7±85.7	7	476.4±79.3[a]	12	609.6±178.4	12	535.3±96.6

Values are means ± SDs. [a]P<0.01 vs. +/+-basal diet group. [b]P<0.05, [c]P<0.01 vs. +/*fa*-basal diet group.

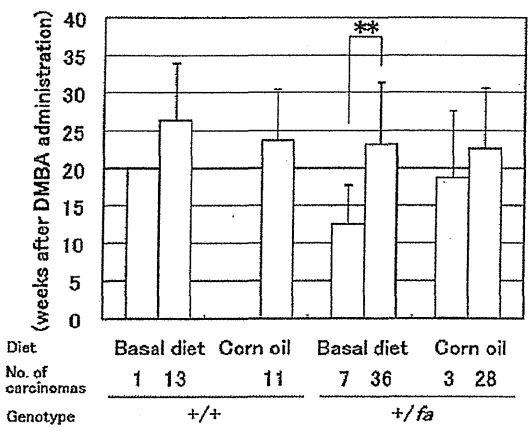

Figure 4. Latency of sub-classified mammary carcinomas based on the morphological phenotypes. Gray bars, moderately/poorly differentiated carcinoma with atypia; open bars, well-differentiated carcinoma without distinct atypia. **P<0.05.

β- and aromatase-immunohistochemistry, frozen sections of 1, 0, 3 and 3 moderately/poorly differentiated carcinomas from the +/+-basal diet, +/+-corn oil diet, +/*fa*-basal diet and +/fa-corn oil diet groups, respectively, and 2, 4, 1 and 2 well differentiated carcinomas each were used (Fig. 5A and B). Although no apparent differences in the positive intensities or positive cell ratio for ER β and aromatase were found among the combinations with two phenotypes and two diets in the immunohistochemistry, immunoblot analyses revealed a decrease in ER β expression levels in moderately/poorly differentiated carcinomas (Fig. 5C and D) and decreased expression levels of aromatase in mammary carcinomas regardless of their phenotypes and diets as compared to the normal mammary tissue (Fig. 5C and E).

To examine the relation of intracellular signaling cascades responsive to extracellular stimuli, such as growth factors or cytokines, with the mammary carcinoma phenotypes, immunoblot analyses for phosphorylation levels of ERK1/2

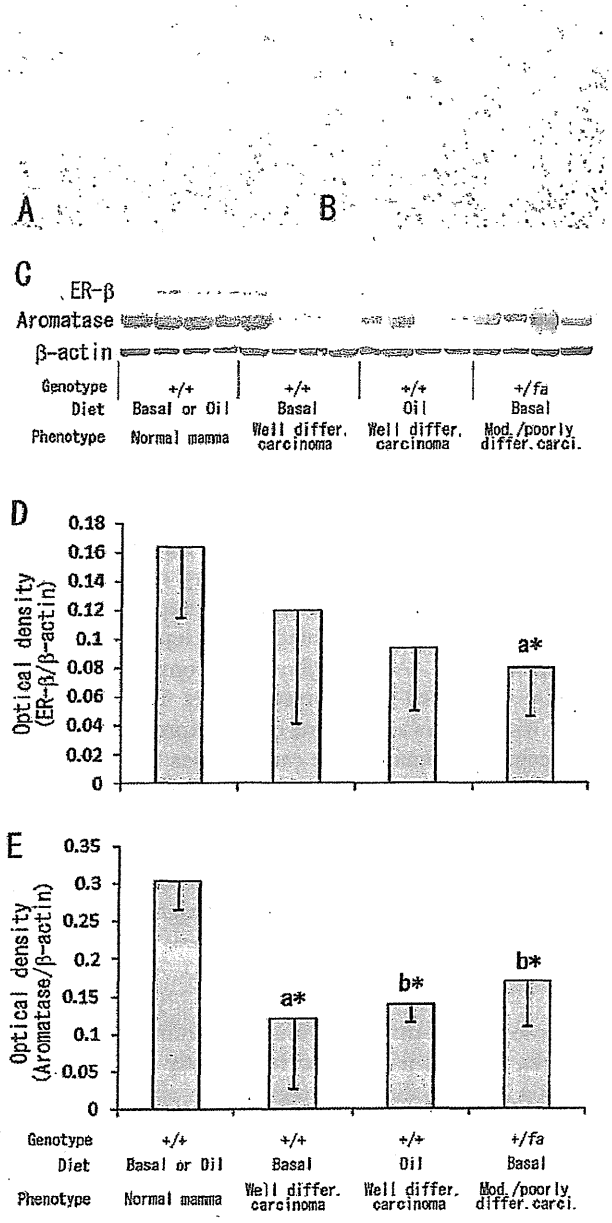

Figure 5. Expression of estrogen receptor (ER) β and aromatase in mammary carcinomas. Immunohistochemistry for (A) ER β, showing nuclear positivity in carcinoma cells of a well differentiated carcinoma in a +/+ rat fed basal diet; (B) aromatase, showing cytoplasmic positivity in presumed myoepithelial and/or mesenchymal cells of a moderately/poorly differentiated carcinoma in a +/*fa* rat fed basal diet. Western blotting for ER β and aromatase (C), and semi-quantitative optical density of ER-β (D) and aromatase (E). ^{a*}P<0.05, ^{b*}P<0.01 vs. normal mammary tissue.

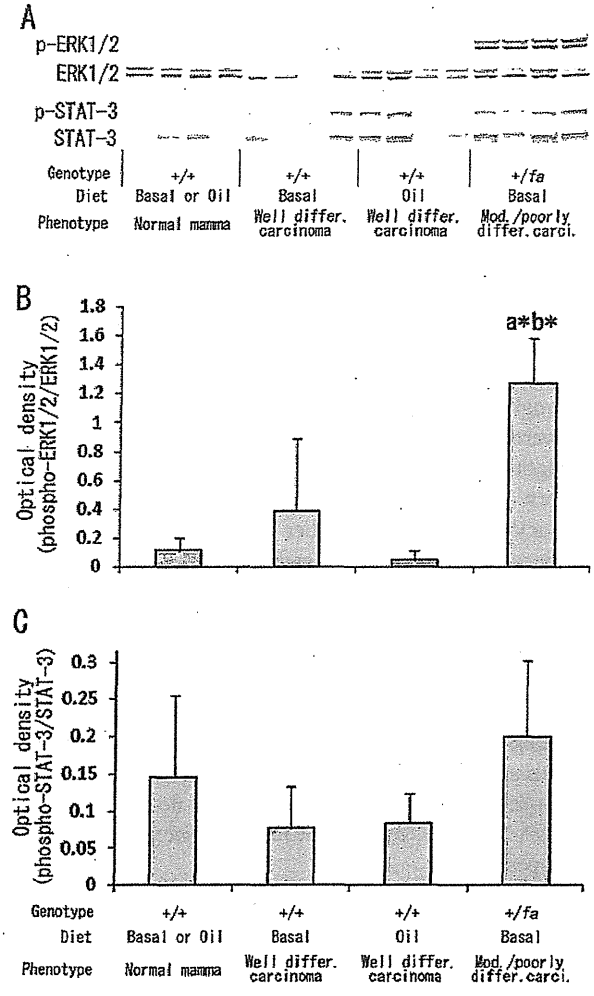

Figure 6. Phosphorylation levels of extracellular signal-regulated kinase (ERK)1/2 and signal transducer and activator of transcription (STAT)3 in mammary carcinomas. Western blotting for phospho-ERK1/2, ERK1/2, phospho-STAT3 and STAT3 (A) and semi-quantitative optical density of phospho-ERK1/2 (B) and phospho-STAT3 (C) compared to those of ERK1/2 and STAT3, respectively. ^{a*}P<0.05 vs. well differentiated carcinomas in +/+ rats fed basal diet, and ^{b*}P<0.01 vs. normal mammary tissue in +/+ rats fed basal or corn oil diet and well-differentiated carcinomas in +/+ rats fed corn oil diet.

and STAT3 were performed, and activation of the ERK1/2 signaling pathway but not STAT3 was demonstrated in moderately/poorly differentiated carcinomas with atypia as compared to normal mammary tissue and well differentiated carcinomas without distinct atypia (Fig. 6). No influence of corn oil diet was found with regard to either ERK1/2 or STAT3 activation (Fig. 6).

Serum biochemistry. Data for serum levels of triglycerides, total cholesterol and glucose at terminal sacrifice are summarized in Table V. Although triglyceride and total cholesterol levels declined or showed a tendency for decline and glucose levels were elevated by the corn oil diet in the +/*fa* genotype, no apparent change in these three parameters was observed in +/+ controls. No obvious differences in these parameters were found between the genotypes. Serum leptin levels in the +/*fa*-basal diet and the +/*fa*-corn oil diet groups were comparable to those in the +/+-counterparts, whereas corn oil diet elevated serum leptin levels in the +/*fa* genotype with a similar tendency for elevation in the +/+ genotype (Table V). Serum adiponectin levels in the +/*fa*-basal diet group were lower than in the +/+-basal diet group, and corn oil diet caused elevation only in the +/*fa* case. Serum IGF-I levels were lower in the +/+-corn oil diet than +/+-basal diet groups, but no change was observed with the +/*fa* genotype. There was no evident variation noted in serum insulin levels among the groups.

Discussion

The present DMBA-induced mammary carcinogenesis study using heterozygous (+/*fa*) and wild-type (+/+) lean Zucker rats revealed higher susceptibility of +/*fa* rats to DMBA induction of mammary tumors than +/+ rats, and also differences in histopathological phenotypes of the induced carcinomas. In particular, the latency periods of mammary carcinoma development in +/*fa* rats fed basal or corn oil diet appeared shorter than those in +/+ rats and the incidences and multiplicities of mammary carcinomas were increased or showed a tendency for increase in the early stages, with a greater percentage of more advanced cancer at the termination.

Although the body weight of +/+ and +/*fa* rats fed corn oil diet were higher than those of the rats fed basal diet, the body weight differences between +/+ and +/*fa* rats fed basal diet or corn oil diet were significantly smaller. Therefore, the short latency periods and the higher incidence and multiplicity of mammary carcinomas in the early stages in +/*fa* rats were considered not to be directly due to body weight change. On the other hand, in our preliminary study, serum leptin concentration at 7 weeks of age was ~140 pg/ml in +/*fa*, higher ($P<0.01$) than ~80 pg/ml (18). These results indicated that the increased susceptibility of +/*fa* rats to DMBA-induced mammary carcinogenesis might be at least partly associated with higher leptin levels at the initiation stage. Hyperleptinemia in juvenile stages of +/*fa* rats gradually normalized and no difference in serum leptin level was found at the terminal sacrifice between the genotypes.

Histopathologically, adenocarcinomas in +/*fa* rats were more likely to present characteristic features such as moderate/poor differentiation, nuclear atypia, prominent interstitial cell proliferation and low ER α positivity. Expression levels of aromatase were decreased in mammary carcinomas regardless of the phenotype as compared to normal mammary tissue. On the other hand, leptin receptor and leptin were expressed with various intensities and no distinct differences were found between carcinomas with and without atypia. Although the cause of the lowered ER α protein expression in the moderately/poorly differentiated carcinomas with atypia is not clear, one possibility is that mammary epithelial cells of +/*fa* rats were initiated under conditions without estrogen-dependence but with close dependence on other growth factors, such as leptin or EGFR (10,23). Activation of the mitogen-activated protein kinase (MAPK) system has been demonstrated in moderately/poorly differentiated carcinomas with atypia. Thus, Thordarson *et al* (24) reported that *N*-methyl-*N*-nitrosourea (MNU)-induced mammary carcinomas in ovariectomized Sprague-Dawley rats showed a more aggressive phenotype with a significant increase in MAPK activity (phosphorylation) as compared to carcinomas in intact rats, suggesting a relationship between loss of estrogen-dependence and growth. Also, in an estrogen-non-responsive human breast cancer cell line, MAPK activity was found to be increased as compared to the original estrogen-dependent sample, suggesting that increased activity of MAPK may contribute to the estrogen non-responsive growth phenotype (25).

Epidemiologically, breast cancer rates among pre-and perimenopausal ages are reported to be higher among US-born Chinese than those born in foreign countries, and similar findings were found in Filipina women as well, to the extent that contemporary rates may equal or exceed those of non-Hispanic Whites, indicating that becoming acculturated to the western lifestyle might be a breast cancer risk factor to some younger Asian women (26). Plasma leptin levels were demonstrated to be twice as high in US-born South Asian (India, Bangladesh, Sri Lanka) women aged 18-30 years than in European women (27), presumably related to the increasing rate of breast cancer. In addition, in certain Asian countries, such as India and Singapore, breast cancer patients present at a younger age, with more advanced stage and fewer estrogen-ER-positive tumors, as compared to western countries (28,29). Therefore, we propose that the present DMBA-induced mammary carcinogenesis in +/*fa* lean Zucker rats may be a useful model of increasing breast cancer in younger Asian women.

A further significant finding of the present DMBA-induced mammary carcinogenesis study in +/*fa* and +/+ rats with and without 10% corn oil diet is that elevation of serum leptin level may contribute to the growth of mammary tumors. In our preliminary study, corn oil diet, similarly prepared as in the present study, significantly elevated serum leptin concentrations of 12-week-old +/+ and +/*fa* rats as compared to basal diet, as also confirmed in the present study. These data are consistent with the previous reports of overexpression of leptin and its receptor in human breast cancer cases (30,31), and in *in vitro* studies revealing that leptin can stimulate breast cancer cell proliferation (23,32). From epidemiological studies, it is well recognized that obesity increases the risk of breast cancer in postmenopausal women, with a suggested association with menstrual and reproductive factors (33) or higher circulating levels of leptin. However, the mechanisms have yet to be fully elucidated (34,35).

In conclusion, +/*fa* rats in the present study proved more susceptible to DMBA-induced mammary carcinogenesis than +/+ controls, and this might be at least partly related to the higher leptin levels in the early stages. Corn oil diet possibly contributed to the growth of mammary tumors via elevated serum leptin levels. In addition, an aggressive phenotype of carcinoma, in which MAPK cascade but not estrogen signaling was activated, was found predominantly in +/*fa* rats. Further studies are required to examine the mechanisms of MAPK activation for mammary carcinogenesis in +/*fa* rats.

Acknowledgements

The present study was supported in part by a grant-in-aid for Cancer Research (19-2) and the Third-Term Comprehensive Control Research for Cancer (H22-G-014) from the Ministry of Health, Labour and Welfare of Japan. The authors thank Dr Malcolm A. Moore for revision of the text and Ms. Ayako Kaneko and Ms. Satomi Kohno for their expert technical assistance. We also thank the National Cancer Center Research Core Facility for some of the analyses in this study. The Core Facility was supported by the National Cancer Center Research and Development Fund (23-A-7).

References

1. van den Brandt PA, Spiegelman D, Yaun SS, *et al*: Pooled analysis of prospective cohort studies on height, weight, and breast cancer risk. Am J Epidemiol 152: 514-527, 2000.

2. Lahmann PH, Hoffmann K, Allen N, *et al*: Body size and breast cancer risk: findings from the European Prospective Investigation into Cancer and Nutrition (EPIC). Int J Cancer 111: 762-771, 2004.
3. Reeves GK, Pirie K, Beral V, Green J, Spencer E and Bull D: Cancer incidence and mortality in relation to body mass index in the Million Women Study: cohort study. BMJ 335: 1134, 2007.
4. Iwasaki M, Otani T, Inoue M, Sasazuki S and Tsugane S: Body size and risk for breast cancer in relation to estrogen and progesterone receptor status in Japan. Ann Epidemiol 17: 304-312, 2007.
5. Key TJ, Appleby PN, Reeves GK, *et al*: Body mass index, serum sex hormones, and breast cancer risk in postmenopausal women. J Natl Cancer Inst 95: 1218-1226, 2003.
6. Auwerx J and Staels B: Leptin. Lancet 351: 737-742, 1998.
7. Wu MH, Chou YC, Chou WY, *et al*: Circulating levels of leptin, adiposity and breast cancer risk. Br J Cancer 100: 578-582, 2009.
8. Soma D, Kitayama J, Yamashita H, Miyato H, Ishikawa M and Nagawa H: Leptin augments proliferation of breast cancer cells via transactivation of HER2. J Surg Res 149: 9-14, 2008.
9. Saxena NK, Taliaferro-Smith L, Knight BB, *et al*: Bidirectional crosstalk between leptin and insulin-like growth factor-I signaling promotes invasion and migration of breast cancer cells via transactivation of epidermal growth factor receptor. Cancer Res 68: 9712-9722, 2008.
10. Cirillo D, Rachiglio AM, la Montagna R, Giordano A and Normanno N: Leptin signaling in breast cancer: an overview. J Cell Biochem 105: 956-964, 2008.
11. Chua SC Jr, Chung WK, Wu-Peng XS, *et al*: Phenotypes of mouse diabetes and rat fatty due to mutations in the OB (leptin) receptor. Science 271: 994-996, 1996.
12. Bray GA: The Zucker-fatty rat: a review. Fed Proc 36: 148-153, 1977.
13. Rayner DV, Dalgliesh GD, Duncan JS, Hardie LJ, Hoggard N and Trayhurn P: Postnatal development of the ob gene system: elevated leptin levels in suckling fa/fa rats. Am J Physiol 273: R446-R450, 1997.
14. Lee WM, Lu S, Medline A and Archer MC: Susceptibility of lean and obese Zucker rats to tumorigenesis induced by *N*-methyl-*N*-nitrosourea. Cancer Lett 162: 155-160, 2001.
15. Hakkak R, Holley AW, Macleod SL, *et al*: Obesity promotes 7,12-dimethylbenz(a)anthracene-induced mammary tumor development in female zucker rats. Breast Cancer Res 7: R627-R633, 2005.
16. Hakkak R, MacLeod S, Shaaf S, *et al*: Obesity increases the incidence of 7,12-dimethylbenz(*a*)anthracene-induced mammary tumors in an ovariectomized Zucker rat model. Int J Oncol 30: 557-563, 2007.
17. de Assis S, Wang M, Goel S, Foxworth A, Helferich W and Hilakivi-Clarke L: Excessive weight gain during pregnancy increases carcinogen-induced mammary tumorigenesis in Sprague-Dawley and lean and obese Zucker rats. J Nutr 136: 998-1004, 2006.
18. Cho YM, Imai T, Takami S, Ogawa K and Nishikawa A: Female heterozygous (*+/fa*) Zucker rats as a novel leptin-related mammary carcinogenesis model. J Toxicol Sci 37: 1025-1034, 2012.
19. Phillips MS, Liu Q, Hammond HA, *et al*: Leptin receptor missense mutation in the fatty Zucker rat. Nat Genet 13: 18-19, 1996.
20. Imai T, Cho YM, Hasumura M and Hirose M: Enhancement by acrylamide of *N*-methyl-*N*-nitrosourea-induced rat mammary tumor development-possible application for a model to detect co-modifiers of carcinogenesis. Cancer Lett 230: 25-32, 2005.
21. Cho YM, Imai T, Hasumura M and Hirose M: Lack of enhancement of susceptibility to mammary and thyroid carcinogenesis in rats exposed to DMBA and DHPN following prepubertal iodine deficiency. Cancer Sci 97: 1031-1036, 2006.
22. Ip C, Carter CA and Ip MM: Requirement of essential fatty acid for mammary tumorigenesis in the rat. Cancer Res 45: 1997-2001, 1985.
23. Mauro L, Catalano S, Bossi G, *et al*: Evidences that leptin up-regulates E-cadherin expression in breast cancer: effects on tumor growth and progression. Cancer Res 67: 3412-3421, 2007.
24. Thordarson G, Lee AV, McCarty M, *et al*: Growth and characterization of *N*-methyl-*N*-nitrosourea-induced mammary tumors in intact and ovariectomized rats. Carcinogenesis 22: 2039-2047, 2001.
25. Coutts AS and Murphy LC: Elevated mitogen-activated protein kinase activity in estrogen-non responsive human breast cancer cells. Cancer Res 58: 4071-4074, 1998.
26. Gomez SL, Quach T, Horn-Ross PL, *et al*: Hidden breast cancer disparities in Asian women: disaggregating incidence rates by ethnicity and migrant status. Am J Public Health 100 (Suppl 1): S125-S131, 2010.
27. Kalhan R, Puthawala K, Agarwal S, Amini SB and Kalhan SC: Altered lipid profile, leptin, insulin, and anthropometry in offspring of South Asian immigrants in the United States. Metabolism 50: 1197-1202, 2001.
28. Ghumare SS and Cunningham JE: Breast cancer trends in Indian residents and emigrants portend an emerging epidemic for India. Asian Pac J Cancer Prev 8: 507-512, 2007.
29. Lim SE, Back M, Quek E, Iau P, Putti T and Wong JE: Clinical observations from a breast cancer registry in Asian women. World J Surg 31: 1387-1392, 2007.
30. Ishikawa M, Kitayama J and Nagawa H: Enhanced expression of leptin and leptin receptor (OB-R) in human breast cancer. Clin Cancer Res 10: 4325-4331, 2004.
31. Garofalo C, Koda M, Cascio S, *et al*: Increased expression of leptin and the leptin receptor as a marker of breast cancer progression: possible role of obesity-related stimuli. Clin Cancer Res 12: 1447-1453, 2006.
32. Ray A, Nkhata KJ and Cleary MP: Effects of leptin on human breast cancer cell lines in relationship to estrogen receptor and HER2 status. Int J Oncol 30: 1499-1509, 2007.
33. Iwasaki M, Otani T, Inoue M, Sasazuki S and Tsugane S: Role and impact of menstrual and reproductive factors on breast cancer risk in Japan. Eur J Cancer Prev 16: 116-123, 2007.
34. Grossmann ME, Ray A, Nkhata KJ, *et al*: Obesity and breast cancer: status of leptin and adiponectin in pathological processes. Cancer Metastasis Rev 29: 641-653, 2010.
35. Hjartaker A, Langseth H and Weiderpass E: Obesity and diabetes epidemics: cancer repercussions. Adv Exp Med Biol 630: 72-93, 2008.

Genetic reconstitution of tumorigenesis in primary intestinal cells

Kunishige Onuma[a], Masako Ochiai[a], Kaoru Orihashi[a], Mami Takahashi[b], Toshio Imai[b], Hitoshi Nakagama[a], and Yoshitaka Hippo[a,1]

[a]Division of Cancer Development System and [b]Central Animal Division, National Cancer Center Research Institute, Tokyo 104-0045, Japan

Edited by Bert Vogelstein, Johns Hopkins University, Baltimore, MD, and approved May 28, 2013 (received for review December 17, 2012)

Animal models for human colorectal cancer recapitulate multistep carcinogenesis that is typically initiated by activation of the Wnt pathway. Although potential roles of both genetic and environmental modifiers have been extensively investigated in vivo, it remains elusive whether epithelial cells definitely require interaction with stromal cells or microflora for tumor development. Here we show that tumor development could be simply induced independently of intestinal microenvironment, even with WT murine primary intestinal cells alone. We developed an efficient method for lentiviral transduction of intestinal organoids in 3D culture. Despite seemingly antiproliferative effects by knockdown of adenomatous polyposis coli (*APC*), we managed to reproducibly induce *APC*-inactivated intestinal organoids. As predicted, these organoids were constitutively active in the Wnt signaling pathway and proved tumorigenic when injected into nude mice, yielding highly proliferative tubular epithelial glands accompanied by prominent stromal tissue. Consistent with cellular transformation, tumor-derived epithelial cells acquired sphere formation potential, gave rise to secondary tumors on retransplantation, and highly expressed cancer stem cell markers. Inactivation of *p53* or phosphatase and tensin homolog deleted from chromosome 10, or activation of *Kras*, promoted tumor development only in the context of *APC* suppression, consistent with earlier genetic studies. These findings clearly indicated that genetic cooperation for intestinal tumorigenesis could be essentially recapitulated in intestinal organoids without generating gene-modified mice. Taken together, this in vitro model for colon cancer described herein could potentially provide unique opportunities for carcinogenesis studies by serving as a substitute or complement to the currently standard approaches.

colon carcinogenesis | shRNA | primary culture | Matrigel | validation

Accumulation of multiple genetic alterations underlies colon carcinogenesis, in which inactivation of adenomatous polyposis coli (*APC*) is an initiating event leading to the development of adenoma in most sporadic cases (1). Both *APC* inactivation and an activating mutation in the *CTNNB1* gene encoding β-catenin result in β-catenin accumulation through inhibition of its degradation, leading to constitutive activation of the Wnt pathway that is transcriptionally regulated by the β-catenin/transcription factor 4 (TCF) complex (2).

Widely used animal models for colorectal cancer (CRC) recapitulate tumor development in a similar manner. One is a mouse genetic model with a mutant allele of *APC*. Typically, multiple adenomas spontaneously develop predominantly in the small intestine through inactivation of the remaining allele (3, 4). The other is a chemically induced carcinogenesis model. Administration of azoxymethane (AOM) or a dietary carcinogen, 2-amino-1-methyl-6-phenylimidazo [4,5-*b*] pyridine (PhIP), recapitulates colon carcinogenesis in rodents by introducing an activating mutation in *CTNNB1* (5, 6) or inactivating *APC*, by mutation (7) or post-transcriptional down-regulation by overexpressed staphylococcal nuclease and tudor domain containing 1 (*SND1*) (8). Potential roles of genetic or environmental factors have been extensively investigated with these models. For instance, disruption of *p53* (9, 10) or phosphatase and tensin homolog deleted from chromosome 10 (*PTEN*) (11, 12) or induction of oncogenic *Kras* (13–15) significantly promoted intestinal tumorigenesis only in the context of *APC* loss. Protumorigenic effects by active inflammation have been demonstrated by inducing colitis with dextran sodium sulfate (DSS) (16). Conversely, critical roles of microflora and basal inflammation underlying tumorigenesis were also demonstrated by genetic ablation of *Myd88* (17) and *STAT3* (18), key genes in the innate immunity and inflammation, respectively.

Recent genomic and expression profile analyses have revealed a huge number of genes with mutation, deletion, or aberrant expression in human CRC (19, 20). Forward genetic screens in mice have also identified a number of genes potentially involved in intestinal tumorigenesis (21). Candidate genes for CRC have been usually validated through generation of gene-modified mice. However, it might be unrealistic to take this approach for very many genes, given the amount of time and work required for the analysis of each gene. This situation is especially true if generation of conditional KO mice and intercrossing between multiple strains becomes necessary. Alternatively, functional analyses of the genes have been widely conducted in colon cancer cell lines and fibroblasts to investigate the relevance in tumor progression and to determine oncogenic potential, respectively. However, the results might not be directly extrapolated to early stages of intestinal tumorigenesis, underscoring the definite requirement for simple validation methods in normal intestinal cells.

Given that intestinal stem cells efficiently give rise to adenoma on activation of the Wnt pathway in vivo (22, 23), we postulated that a similar approach might induce tumor development in vitro, although the requirements of intestinal microenvironment remained elusive. With recent advances in long-term culture of intestinal stem cells (24), we set out to suppress *APC* in intestinal organoids with a lentivirus. We generated tumors from intestinal organoids, independently of the in vivo setting and without using gene-modified mice. Representative genetic cooperation for tumorigenesis could be recapitulated by taking this approach, likely establishing an in vitro model for CRC.

Results

Lentivirus-Based Efficient and Stable Gene Delivery to Intestinal Organoids. To reconstitute tumorigenesis in vitro, stem cells need to be stably transduced. We adopted lentiviral gene delivery for its high infection efficiency to primary cells, including quiescent stem cells (25). However, it was revealed that Matrigel inhibited viral transduction of intestinal epithelial cells (IECs) in 3D culture, despite its definite requirement for survival. To satisfy both the presence of Matrigel and accessibility to lentiviral

Author contributions: H.N. and Y.H. designed research; K. Onuma, M.O., K. Orihashi, and Y.H. performed research; M.T. contributed new reagents/analytic tools; T.I. analyzed data; and Y.H. wrote the paper.

The authors declare no conflict of interest.

This article is a PNAS Direct Submission.

[1]To whom correspondence should be addressed. E-mail: yhippo@ncc.go.jp.

This article contains supporting information online at www.pnas.org/lookup/suppl/doi:10.1073/pnas.1221926110/-/DCSupplemental.

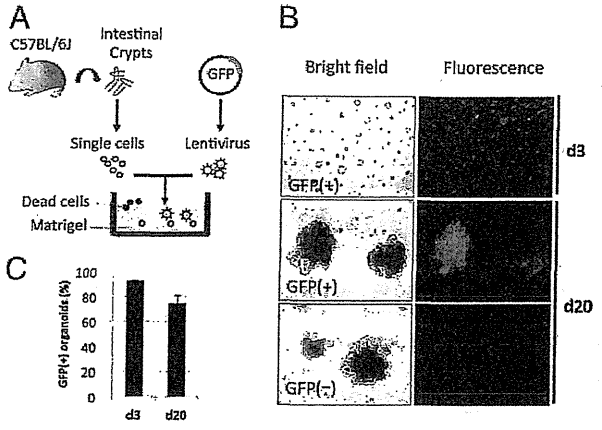

Fig. 1. Stable gene transduction of IECs in 3D culture. (*A*) Schematic diagram for lentiviral infection. Intestinal crypts isolated from C57BL/6J mice were dissociated into single cells and incubated with lentiviral particles encoding GFP for 16 h on Matrigel. (*B*) Stable and efficient transduction of organoids. Transduced organoids at day 3, at 40× magnification (*Top*). At day 20, transduced organoids consisting of GFP-positive cells (*Middle*). A non-GFP vector gave rise to only faint auto-fluorescence by dead cells at 100× magnification (*Bottom*). Representative images are shown. (*C*) Transduction efficiency to intestinal cells. Rate for GFP-positive organoids without drug selection is shown. GFP-positive and -negative organoids were counted under a microscope 48 h after the infection (day 3) or second subculture (day 20). Mean ± SD ($n = 3$) is shown.

particles, we coincubated dissociated single cells and viral particles on Matrigel (Fig. 1*A*), which achieved high transduction efficiency (Fig. 1*B*). About half of the cells composing organoids were viable, and ~20% of them attached to Matrigel with or without viral particles (Fig. S1), whereas no dead cells were observed on Matrigel. Attached cells readily developed into tiny circular organoids at day 3 (Fig. 1*B*), implying this procedure might enable preferentially capture intestinal cells of a highly proliferative nature. Even without drug selection, the GFP-positive rate was as high as 93% at day 3, which fell to 75% at day 20 (Fig. 1*C*), presumably due to slightly adverse effects by viral integration. Many organoids consisted of only GFP-positive cells at day 20, even after two rounds of subculture (Fig. 1*B*). Given the rapid turnover rate of IECs (24), we reasoned that organoids were likely reconstituted by stably transduced stem cells.

Wnt Pathway Activation in Organoids Transduced with Multiple Clones of shRNA Against *APC*. With this efficient technique, we introduced a total of five clones of potent shRNA against *APC* (shAPC) (Fig. S2*A*) individually into organoids. With a routine schedule for 3D culture (Fig. S2*B*), however, we frequently failed in propagation for any shAPC clone tested, even under drug selection (Fig. S2*C*), suggesting adverse effects by *APC* knockdown in vitro. In contrast, introduction of potent shp53 or shPTEN (Fig. S2*D*) resulted in steady propagation of organoids (Fig. 2*A*), which spontaneously became puro-resistant, suggesting a growth advantage of inactivating *p53* or *PTEN*. We later found that cointroducing all of the five shAPC clones together (hereafter referred to as shAPCs) reproducibly gave rise to rounded cystic organoids, which dominated the population over time (Fig. 2*A*; Fig. S2*C*). Similar structures have been previously documented for organoids from *APC*-deficient adenoma (26, 27), suggesting a link between the morphology and *APC* loss. However, we assumed that this might not be necessarily the case, because we knew that cystic shape could be induced independent of *APC* knockdown (e.g., under stressed culture conditions including freeze/thaw, drug selection, or too stringent dissociation), which prompted us to characterize the cystic organoids with shAPCs in more detail. We found that they were puro-resistant and indeed suppressed for expression of *APC* (Fig. S2*D*). In thin sections, they lost physiological properties such as polarity (Fig. 2*B*), differentiation (Fig. 2*C*), and cellular turnover (Fig. 2 *B* and *C*), consistent with perturbed differentiation and migration associated with *APC* inactivation (28). In addition, β-catenin accumulation indicative of Wnt pathway activation was evident (Fig. 2*D*), which was also confirmed by qPCR analysis demonstrating up-regulation of *Axin2* (Fig. 2*E*), a specific target of the β-catenin/TCF complex (29). These observations implied that the organoids with shAPCs might be essentially similar, if not identical, to those derived from *APC*-deficient adenoma.

Induction of Tumors from Organoids by RNAi-Mediated Suppression of *APC*. We next investigated whether suppression of *APC* in organoids could also lead to tumor development, as observed in adenoma in vivo. After 4 wk of culture, organoids with shAPCs corresponding to 5×10^5 cells were mixed with Matrigel and injected into nude mice. At 6 wk after injection, round and solid flesh-colored nodules frequently developed (Fig. 3*A*). They were characterized by epithelial glands and prominently infiltrated stromal cells (Fig. 3*B*). Active proliferation of epithelia was verified by high Ki-67 labeling index and inferred from β-catenin accumulation (Fig. 3*C*). Based on these features common to intestinal tumors, we classified them as "tumors." In contrast, organoids with the vector control gave rise to no nodules at all or small flat nodules with a gelatinous appearance, if any (Fig. 3*A*). As they histologically lacked epithelial glands (Fig. 3*B*), we classified them as "Matrigel plugs." In the absence of shAPCs, no tumor was induced by shp53 and/or shPTEN or from *p53*- and *PTEN*-deficient organoids (Fig. S3; Table 1), in line with earlier studies in vivo (11, 12, 30, 31). In some cases, organoids with

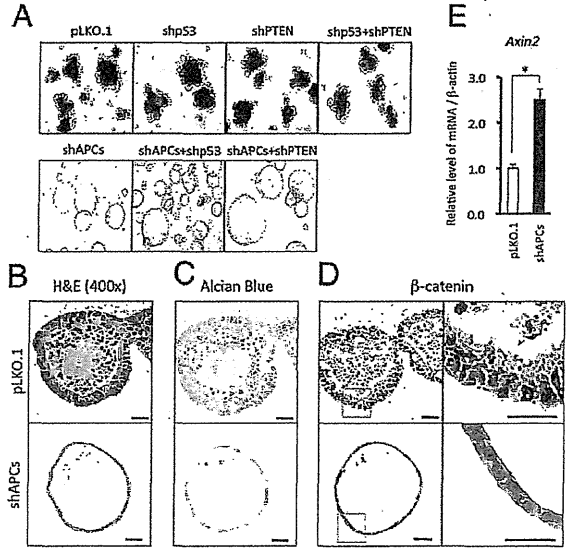

Fig. 2. RNAi-mediated suppression of *APC* in intestinal organoids. (*A*) Organoids transduced with various shRNA(s). Representative images at 4 wk after transduction are shown. Large rounded cysts were induced exclusively in the presence of shAPCs. pLKO.1 is an empty vector. (*B–D*) Transduced organoids in thin section. Serial sections were stained with H&E (*B*), Alcian blue (*C*), and β-catenin antibody (*D*). In organoids with shAPCs, intraluminal debris due to physiological turnover of intestinal cells is lost. Paneth cells stained red (*B*) and mucus stained blue (*C*) also became absent. Localization of β-catenin shifted from membrane to cytoplasm and nucleus (*D*). *Insets* in the left panel are enlarged in the right panel. (Scale bar, 20 μm.) (*E*) qPCR analysis of *Axin2* in transduced organoids. Relative expression level of mRNA to *β-actin* is shown. Mean ± SD ($n = 3$) is shown; $^*P < 0.01$.

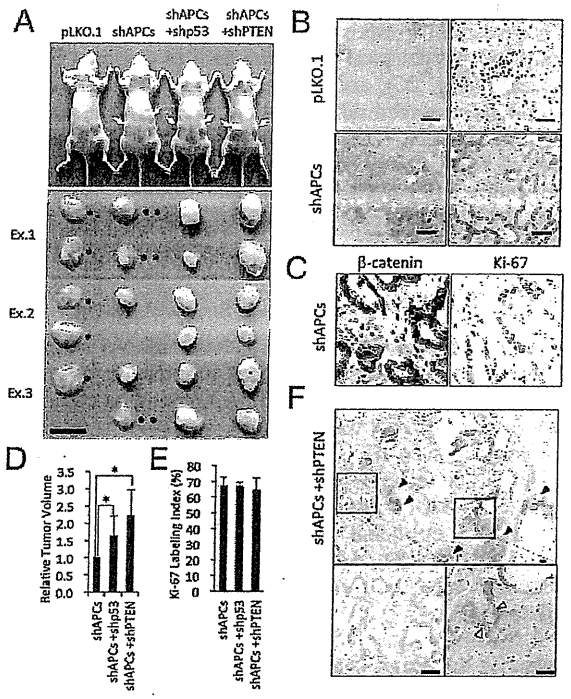

Fig. 3. RNAi-mediated induction of tumors from WT organoids. (*A*) s.c. tumors developed from injected organoids. Palpable nodules in nude mice (arrow) at 6 wk after injection (*Upper*). Excised nodules in three representative experiments (Ex.1–3). Matrigel plugs (asterisk), nontumor (double asterisks), or tumors (no asterisk) (*Lower*). (Scale bar, 10 mm.) (*B*) Histological features of the nodules. H&E staining of Matrigel plugs (*Upper*) and tumors with shAPCs alone (*Lower*) at 20× (*Left*) and 200× (*Right*) magnification. (Scale bar, 500 and 50 μm, respectively.) (*C*) Immunohistochemical analyses. Tumors with shAPCs alone stained for β-catenin (*Left*) and Ki-67 (*Right*). (Scale bar, 25 μm.) (*D*) Relative ratio of tumor volume. Mean ± SD ($n = 5$) is shown; $^*P < 0.05$. (*E*) Ki-67 labeling index for tumor epithelia. Mean ± SD ($n = 7$) is shown. (*F*) Alcian blue staining. Tumors with shAPCs+shPTEN were stained. Mucus pools stained in blue (closed arrowhead) in stroma (*Upper*). *Insets* are enlarged in lower panel. Mucus and cellular debris shed into the lumen (*Lower Left*) are leaking (open arrowhead) from the disrupted glands (*Lower Right*). (Scale bar, 50 μm.)

shAPCs alone comprised nodules resembling Matrigel plugs, but having focal white spots inside (Fig. 3*A*). We classified them as "nontumor," based on too low a proportion of epithelial cells. Thus, tumors were tentatively defined as nodules replacing coinjected Matrigel with proliferating epithelial glands at 6 wk after injection. By applying this criteria, the tumor development rate by shAPCs alone was 63% (=7/11), 5 cases for both sides and 2 cases for either side, among 11 cases (Table 1). These results suggested that *APC* suppression might be integral but not always sufficient for tumor development from organoids, consistent with earlier studies in vivo (17, 18, 32).

Suppression of *p53* or *PTEN* Promotes *APC*-Dependent Tumorigenesis from Organoids. Many gene-modified mice have been crossed with *APC* mutant mice to evaluate their impact on carcinogenesis, in which common readouts were multiplicity, size, and histology of the tumors. We wondered if similar analysis could be feasible at the cellular level. By cointroducing shp53 or shPTEN with shAPCs into organoids (Fig. 2*A*), tumor development was observed for both sides of nude mice in all of the cases tested (Fig. 3*A*; Table 1). Similar results were obtained by introduction of shAPCs into *p53*- (Fig. S3) and *PTEN*-deficient organoids (Table 1). A significant increase in tumor size was also observed (Fig. 3*D*), but an increase was not observed in proliferation index (Fig. 3*E*). No remarkable effects were detected in histological features, including mucus pool formation (Fig. 3*F*), tumor gland morphology (Fig. S4*A*), and β-catenin accumulation (Fig. S4*B*). Taken together, cooperation for tumorigenesis between *APC* loss and inactivation of either *p53* (9, 10) or *PTEN* (11, 12) could be recapitulated in tumors as an increase in size and development rate. We also verified that organoid culture was conducted in a stromal cell–free condition (Fig. S5), confirming tumorigenesis was indeed achieved with IECs alone.

Significant Acceleration of *APC*-Dependent Tumorigenesis from Organoids by *Kras* Activation. To reconstitute somatic mutation of *Kras*, which is frequent in human CRC (19), we deleted a stop codon flanked by two loxP elements [Lox-Stop-Lox (LSL)] blocking the expression of $Kras^{G12D}$ by lentiviral Cre-mediated recombination (33) in IECs from $Kras^{LSLG12D/+}$ mice (34, 35). Successful deletion was confirmed by detecting the "1-loxP" fragment (35) in genomic PCR (Fig. 4*A*). Amplification of the LSL cassette revealed its partial and complete deletion in organoids with Cre and shAPCs+Cre, respectively (Fig. 4*A*). On $Kras^{G12D}$ expression, active Ras enriched (Fig. 4*B*) without affecting the morphology of the organoids (Fig. 4*C*), verifying specific activation of Ras but not the Wnt pathway. We then asked whether a synergy between oncogenic *Kras* and *APC* loss in intestinal tumorigenesis (13–15) could be recapitulated in our model. Strikingly, organoids with shAPCs+Cre gave rise to tumors on both sides so rapidly that the nude mice became moribund at 2 wk after injection (Fig. 4*D*) in 11 of 11 cases (Fig. 4*E*). They typically appeared red, indicative of active angiogenesis and hemorrhage, and contained cystic dilatation due to retention of serous fluid (Fig. 4*D*). Compared with organoids with shAPCs alone, a significant increase in tumor size was observed (Fig. 4*F*). Cre did not synergize with shAPCs in $Kras^{+/+}$ organoids (Fig. S6), ruling out the possibility of direct synergy between Cre and shAPCs. Tumor glands became more densely packed with morphological alteration from an irregular cystic structure (Fig. 5 *B* and *E*) to a tubular or papillary structure (Fig. 5 *C* and *F*). Destruction of glands leading to mucus pool formation (Fig. 5*H*) disappeared, despite retained mucus production ability (Fig. 5*I*). Given no effects on both cell proliferation (Figs. 4*G* and 5 *K* and *L*) and the magnitude of β-catenin accumulation (Fig. 5 *N* and *O*), $Kras^{G12D}$ might have induced tumor growth through histological alterations. Thus, the synergy was successfully recapitulated in tumors as an increase in size and development rate and alteration in histology.

Marginal Effects by *Kras* Activation Alone on Tumorigenesis from Organoids. We also characterized nodules with either of shAPCs or $Kras^{G12D}$ at 2 wk postinjection for reference, although this was too early for the correct diagnosis. If the criteria for tumors were automatically applied, tumor-positive cases were seven of seven for shAPCs, three of seven for $Kras^{G12D}$, and zero of seven for pLKO.1 (Fig. 4*E*). Putative tumors induced by $Kras^{G12D}$ contained

Table 1. Summary of tumor development induced by shRNA transduction

Genes/genotypes		V	P	5	5P	A	A5	AP	A5P
shRNA	shAPCs					+	+	+	+
	shp53			+	+		+		+
	shPTEN		+		+			+	+
	pLKO.1	+							
IEC	WT	0/14	0/4	0/5	0/3	7/11	8/8	10/10	1/1
	p53 $^{-/-}$	0/4	0/2	—	—	2/2	—	4/4	—
	PTEN $^{-/-}$	0/1	—	—	—	—	1/1	—	—

—, not tested. V, P, 5, and A depict vector, shPTEN, shp53, and shAPCs, respectively.

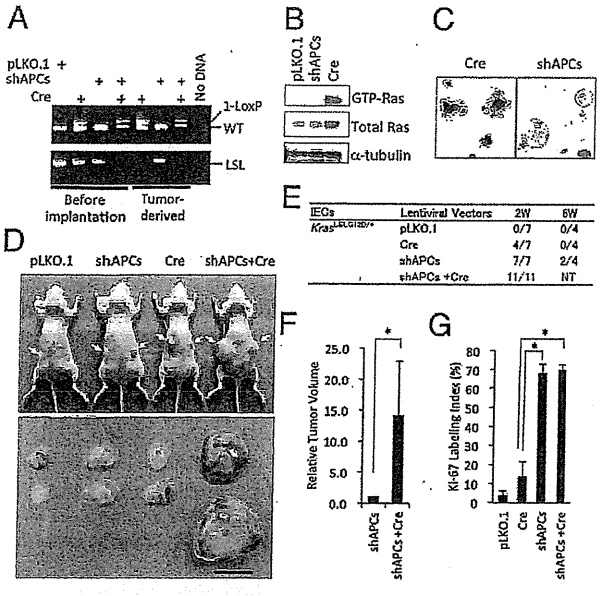

Fig. 4. Synergy between *APC* suppression and *Kras* activation in organoids for tumorigenesis. (*A*) Cre-mediated recombination in vitro. Genomic PCR analysis for WT and recombined allele of *Kras* (*Upper*) and for the LSL cassette (*Lower*). 1-LoxP, single LoxP after the recombination. (*B*) Enrichment of active Ras by induction of $Kras^{G12D}$. Immunoblotting analysis for Ras before (*Middle*) and after (*Top*) GST pulldown assay. α-Tubulin serves as a loading control (*Bottom*). (*C*) Transduced organoids in 3D culture. $Kras^{G12D}$ did not induce cystic shape. (*D*) s.c. tumors in nude mice. Palpable nodules (arrow) at 2 wk postinjection (*Upper*) and corresponding nodules after excision (*Lower*). (Scale bar, 10 mm.) (*E*) Summary of tumor development. Data at 2 and 6 wk after the implantation are shown. NT, not tested. (*F*) relative ratio of tumor volume. Mean ± SD ($n = 7$ each) is shown, $*P < 0.01$. (*G*) Ki-67 labeling index for epithelia in the nodules. Mean ± SD is shown; $*P < 0.01$. pLKO.1 ($n = 3$), Cre ($n = 3$), shAPCs ($n = 7$), and shAPCs+Cre ($n = 7$).

a few glands of ductal or cystic shape (Fig. 5 *A* and *D*), with impaired cell differentiation and proliferation as exemplified by loss of mucus production (Fig. 5*G*) and low Ki-67 index (Figs. 4*G* and 5*J*), respectively. Consistent with the lack of Wnt pathway activation (Fig. 4*C*), β-catenin remained in the membrane (Fig. 5*M*). $Kras^{G12D}$ nodule-derived organoids proved completely deleted for LSL, which had been only partially deleted when injected (Fig. 4*A*), suggesting their transient growth advantage. However, $Kras^{G12D}$ tumors no longer remained at 6 wk after injection (Fig. 4*E*), indicating that *Kras* activation by itself was insufficient for establishment of tumors, consistent with previous studies reporting no effect in the small intestine (13, 14, 36) and induction of only hyperplasia in the colon (15, 37). Also, initial proliferation and eventual extinction might mirror the natural course of aberrant crypt foci (ACF) (38), which are early lesions of the colon highly associated with *Kras* mutation (39).

Acquired Cancer Stem Cell-Like Properties in Tumor-Derived Organoids. As intestinal stem cells (ISCs) were unable to survive in s.c. tissue (Fig. 3*A*), development and maintenance of tumor glands with differentiated and proliferative properties (Fig. 3 *C* and *F*) suggested the emergence of a distinct subpopulation with the ability to self-renew and differentiate. To better characterize the nature of induced tumors, we harvested all of the nodules to conduct organoid cultures and obtained organonids only from tumors. *APC* and *PTEN* were suppressed by corresponding shRNAs (Fig. 6*A*), confirming successful transduction. Tumor-derived organoids proved tumorigenic in all seven cases examined. Notably, tumors from identical cells gave rise to secondary tumors akin to the primary tumors in both magnitude (Fig. 6*B*) and histology (Fig. S7*A*), regardless of genetic background (Fig. S7*B*), further implying the emergence of a cancer stem cell (CSC)-like subpopulation. Sphere-forming potential in suspension culture has been associated with stemness (40). Whereas single cells containing ISCs did not form spheres, tumor-derived organoids yielded spheroids (Fig. 6*C*) in all seven cases examined. Even never-implanted organoids with shAPCs alone formed spheroids (Fig. 6*C*), suggesting induction of the CSC-like properties even before injection into nude mice. Quantitative PCR (qPCR) analysis revealed up-regulation of CSC markers *CD44* and *CD133* (41) but not ISC markers *Lgr5* or *Bmi1* (42) in tumor-derived organoids (Fig. 6*D*). Despite up-regulation of *Axin2* and *CD44* in tumors, *c-Myc* or *CCND1* were not induced, suggesting selective activation of a subset of Wnt target genes toward acquisition of CSC properties. Taken together, these results supported the notion that ISC-containing organoids likely comprised a subpopulation with CSC-like properties through *APC* inactivation.

Discussion

To model human CRC, inactivation of *APC* and subsequent tumor development in the intestine have basically been achieved in mutant or gene-modified mice for *APC* (4). In contrast, we demonstrated that it could also be achieved without a genetically

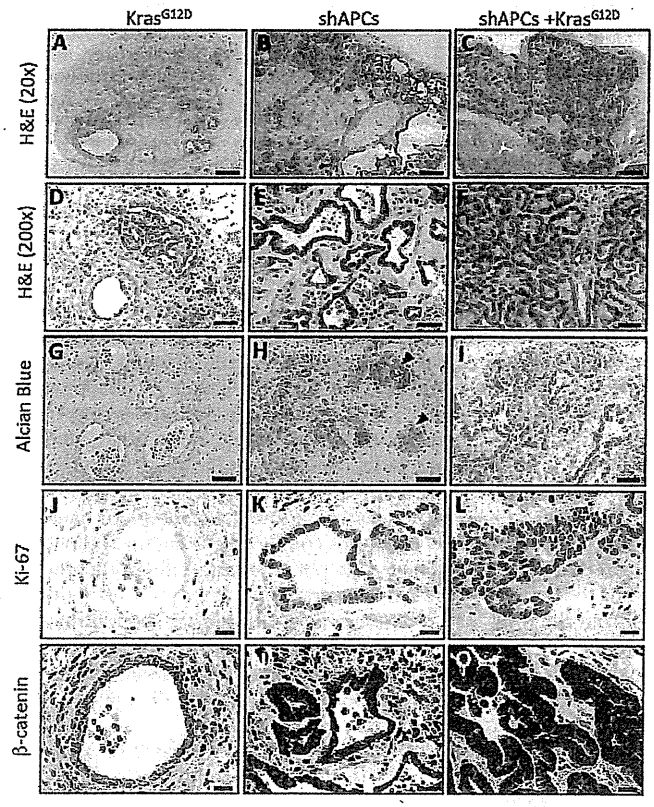

Fig. 5. Histological features of the tumors induced from $Kras^{LSL-G12D/+}$ organoids. (*A–F*) H&E staining at 20× (*A–C*) and 200× (*D–F*) magnification. (Scale bar, 500 and 50 μm, respectively.) (*G–I*) Alcian blue staining. No mucus production (*G*), formation of multiple mucus pool (closed arrowheads) in the stroma (*H*), and mucus confined in the lumen of intact glands (*I*). (Scale bar, 100 μm.) (*J–L*) Immunostaining for Ki-67. Few (*J*) and many (*K* and *L*) positive cells in the tumor glands are observed. (Scale bar, 25 μm.) (*M–O*) Immunostaining for β-catenin. Localized in the membrane (*M*), and accumulated in the cytoplasm or nucleus (*N* and *O*). (Scale bar, 25 μm.) Representative images are shown. Tumors were generated by $Kras^{G12D}$ (*Left*), shAPCs (*Center*), or both (*Right*) from identical cells and harvested at 2 wk after injection.

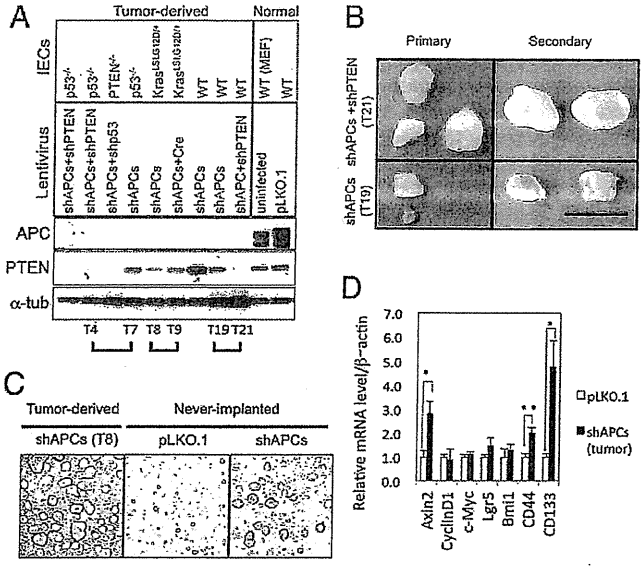

Fig. 6. Induction of cancer stem–like properties in tumors through *APC* suppression. (*A*) *APC* knockdown in tumors. Immunoblotting analysis of tumor-derived organoids for APC and PTEN. Mouse embryonic fibroblast (MEF) and normal IECs are positive controls. T4/7, T8/9, and T19/21 derived from identical primary cells, respectively. (*B*) Serial transplantation of tumors. s.c. tumors T19 (shAPCs) and T21 (shAPCs+shPTEN) in primary sites (*Left*) and corresponding secondary tumors after retransplantation (*Right*). (Scale bar, 10 mm.) (*C*) Sphere-forming assay. Representative images after 2-wk suspension culture are shown. (*D*) qPCR analysis for Wnt target genes and stem cell marker genes. Mean ± SD ($n = 3$) is shown; $^{*}P < 0.01$; $^{**}P < 0.05$.

engineered mouse, independently of intestinal microenvironment, and solely with primary IECs, providing an alternative way to model CRC in vitro. There were several issues to be resolved in the course of developing the model. First was to achieve stable transduction of stem cells, instead of gene targeting in embryonic stem (ES) cells. Despite initial technical difficulties, we eventually established a lentivirus-based transduction method, which was as simple as a routine subculture but highly efficient in obtaining stably transduced organoids. This methodological advantage was in sharp contrast to retroviral transduction of only cycling cells, with more complicated procedures but much less efficiency, definitely requiring drug selection to obtain stably transduced organoids (43). Both high infection efficiency and the growth advantage of inactivating tumor suppressors helped us conduct experiments without drug selection, which eliminated its potential side effects and enabled us to use vectors without selection markers or puro-resistant IECs from the *Kras*$^{LSLG12D/+}$ mouse (34). We further showed that Cre-mediated recombination of a floxed allele could be achieved in organoids. Thus, overexpression and knockdown could be simply achieved for many genes in WT IECs and gene disruption in conditionally gene-targeted IECs.

The second was in vitro expansion of *APC*-inactivated organoids. Inactivation of *APC* in the intestine is normally established by a stochastic second hit in heterozygous mice or by complete loss in mice homozygous for a floxed allele in a spatiotemporally regulated manner (22, 44, 45). Although rounded cystic organonids were available by 3D culture of *APC*-deficient adenoma developed in earlier studies (26, 27), *APC* loss and subsequent tumor development have been exclusively achieved in vivo, to which inflammation or interactions within the microenvironment might have played critical roles (17, 18). In some settings, tumor development itself could not be achieved due to organ failure induced immediately after *APC* loss (28). Thus, it was initially unclear whether we could achieve *APC* inactivation in organoids and its subsequent propagation thoroughly in vitro. IECs transduced with shAPC frequently failed to propagate, which might be partially in line with adverse effects caused by acute *APC* loss (28). We incidentally noted that this could be overcome by cointroducing all of the shAPC clones. A possible explanation could be that pooled shAPC clones yielded variations in the magnitude of Wnt activation, thereby increasing the probability of achieving the "just-right" signaling (46). Alternatively, cooperation among off-target effects by pooled clones could have contributed. Although the underlying mechanism remains to be investigated, organoids that grew out indeed carried shAPCs and phenocopied those derived from *APC*-deficient adenoma. Based on the high similarity, we reasoned that propagated organoids with shAPCs might likely be an in vitro equivalent to adenoma. We then took advantage of this situation for further analysis.

The third was the strict definition of tumor in this model, which was definitely required to relate the results to earlier studies in vivo. We tentatively defined tumors as nodules replacing coinjected Matrigel with proliferating epithelial glands at 6 wk postinjection. Only if tumors proved lethal at an earlier point were nodules exceptionally diagnosed on death. Accordingly, nonlethal nodules at 2 wk after injection were not treated as tumors. Acquisition of the potential for sphere formation and serial transplantation and induction of CSC markers were confirmed in tumor-derived organoids, clearly indicating that they had indeed undergone transformation. These results tend to support the validity of our definition of tumors.

With this experimental system, the relevance of known genetic alterations in CRC could be essentially recapitulated, either individually or in the context of *APC* loss, as in *PTEN* loss (11, 12) and *Kras* activation (13–15, 36, 37). With regard to *p53* loss, its genetic cooperation with *APC* loss was negative in the heterogeneous genetic background (31, 47) but proved to be positive in a congenic background (9, 10), consistent with this study. These findings highlight the relevance of conducting the analysis on genetic interaction in exactly the same genetic background as achieved in our model, which otherwise requires multiple backcrossing. Thus, validation of candidate genes or genetic cooperation will be warranted, leading to quick identification of the genes to be prioritized for further investigations from many candidates (19, 20) before, or even without, generation of gene-modified mice. Also, generation of tumors with defined genotypes could be facilitated. The custom-made "genetically clean" cell lines would become valuable resources for identification of effective compounds or therapeutic targets by high-throughput screening or in preclinical studies.

Considering similarities in outcome and approach, our in vitro model might well be comparable to those two types of in vivo studies, in which *APC* was subject to acute deletion in the intestine, rather than studies with the *APC*-heterozygous mutant mouse (15). One is *APC* loss in an Lgr5^{+} stem cell–specific manner, which quickly gives rise to adenoma (22, 26, 48). The other is *APC* loss either focally or entirely in the intestine. Local injection of adenovirus-Cre induced adenoma in the distal colon, although transduction was achieved in only a limited area (44, 45). Cre-mediated inducible and acute loss of APC throughout the intestine led to morbidity within 5 d (28), but the crypts that were rescued by harvesting 2 d after APC loss proved tumorigenic in nude mice (49). In both cases, *APC* inactivation was achieved in gene-modified mice in vivo, presumably by cooperating with the microenvironment. Besides, special conditions such as cell type–specific gene ablation or crypt harvest at specific times were necessary. In contrast, in our model, *APC* inactivation was simply achieved in WT IECs in vitro, without any other type of cells or experimental conditions, obviously facilitating intestinal tumorigenesis studies. As organoid culture is optimized for Lgr5^{+} stem cells (24), it is conceivable that Lgr5^{+} stem cells were predominantly transformed in our model. On the other hand,

lentiviral transduction could also target quiescent stem cells, which could be marked by Bmi1 (42), Lrig1 (50), mTert (51), or HopX (52), in a mutually overlapping but distinct manner. Moreover, even Lgr5$^-$ differentiated cells could dedifferentiate to reacquire stem cell properties and initiate tumorigenesis (49). Thus, there is a possibility that tumor initiation could take place through many different pathways, including reprogramming of nonstem cells. In this regard, our model might provide unique opportunities in addressing this issue in an unbiased way, as the entire process of tumorigenesis could be simply recapitulated without predefined conditions on tumor-initiating cells.

In conclusion, we developed a unique in vitro model for CRC, with which genetic interactions in both tumor initiation and progression will be simply but genuinely analyzed. By serving as an alternative or complement to the standard approaches, it would likely accelerate CRC research.

Materials and Methods

Singly dissociated intestinal cells were lentivirally transduced in vitro. Organoids were maintained for 4 wk in Matrigel and injected into nude mice to evaluate tumorigenicity. Several weeks after the implantation, the tumors were subjected to histological analysis or 3D culture to obtain a pure population of tumor-derived organoids, which were further analyzed by Western blotting, qPCR, and sphere-forming assay. Extended materials and methods are available in *SI Materials and Methods*.

ACKNOWLEDGMENTS. We thank the Core Facility Division and Central Animal Division in the National Cancer Center Research Institute for technical support in histological and animal studies, respectively. We thank Elaine Fuchs for providing LV-Cre pLKO.1, Hiroshi Ohshima for *p53*-mutant mice, and Akira Suzuki for *PTEN* floxed mice. We also thank Ibuki Kobayashi and Sachiko Dobashi for technical assistance. This study was supported by Grants-in-Aid for the Third Term Comprehensive 10-Year Strategy for Cancer Control from the Ministry of Health, Labor and Welfare of Japan and a grant from the Japan Chemical Industry Association Long Range Research Initiative. K. Onuma was a recipient of the Research Resident Fellowship from the Foundation for Promotion of Cancer Research (Japan).

1. Markowitz SD, Bertagnolli MM (2009) Molecular origins of cancer: Molecular basis of colorectal cancer. *N Engl J Med* 361(25):2449–2460.
2. Walther A, et al. (2009) Genetic prognostic and predictive markers in colorectal cancer. *Nat Rev Cancer* 9(7):489–499.
3. Aoki K, Taketo MM (2007) Adenomatous polyposis coli (APC): A multi-functional tumor suppressor gene. *J Cell Sci* 120(Pt 19):3327–3335.
4. Taketo MM, Edelmann W (2009) Mouse models of colon cancer. *Gastroenterology* 136(3):780–798.
5. Tanaka T (2009) Colorectal carcinogenesis: Review of human and experimental animal studies. *J Carcinog* 8:5.
6. Takahashi M, Nakatsugi S, Sugimura T, Wakabayashi K (2000) Frequent mutations of the beta-catenin gene in mouse colon tumors induced by azoxymethane. *Carcinogenesis* 21(6):1117–1120.
7. Nakagama H, Nakanishi M, Ochiai M (2005) Modeling human colon cancer in rodents using a food-borne carcinogen, PhIP. *Cancer Sci* 96(10):627–636.
8. Tsuchiya N, et al. (2007) SND1, a component of RNA-induced silencing complex, is up-regulated in human colon cancers and implicated in early stage colon carcinogenesis. *Cancer Res* 67(19):9568–9576.
9. Halberg RB, et al. (2008) The pleiotropic phenotype of Apc mutations in the mouse: Allele specificity and effects of the genetic background. *Genetics* 180(1):601–609.
10. Halberg RB, et al. (2000) Tumorigenesis in the multiple intestinal neoplasia mouse: Redundancy of negative regulators and specificity of modifiers. *Proc Natl Acad Sci USA* 97(7):3461–3466.
11. Marsh V, et al. (2008) Epithelial Pten is dispensable for intestinal homeostasis but suppresses adenoma development and progression after Apc mutation. *Nat Genet* 40(12):1436–1444.
12. Shao J, Washington MK, Saxena R, Sheng H (2007) Heterozygous disruption of the PTEN promotes intestinal neoplasia in APCmin/+ mouse: Roles of osteopontin. *Carcinogenesis* 28(12):2476–2483.
13. Janssen KP, et al. (2006) APC and oncogenic KRAS are synergistic in enhancing Wnt signaling in intestinal tumor formation and progression. *Gastroenterology* 131(4):1096–1109.
14. Sansom OJ, et al. (2006) Loss of Apc allows phenotypic manifestation of the transforming properties of an endogenous K-ras oncogene in vivo. *Proc Natl Acad Sci USA* 103(38):14122–14127.
15. Haigis KM, et al. (2008) Differential effects of oncogenic K-Ras and N-Ras on proliferation, differentiation and tumor progression in the colon. *Nat Genet* 40(5):600–608.
16. Tanaka T, et al. (2006) Dextran sodium sulfate strongly promotes colorectal carcinogenesis in Apc(Min/+) mice: Inflammatory stimuli by dextran sodium sulfate results in development of multiple colonic neoplasms. *Int J Cancer* 118(1):25–34.
17. Rakoff-Nahoum S, Medzhitov R (2007) Regulation of spontaneous intestinal tumorigenesis through the adaptor protein MyD88. *Science* 317(5834):124–127.
18. Musteanu M, et al. (2010) Stat3 is a negative regulator of intestinal tumor progression in Apc(Min) mice. *Gastroenterology* 138(3):1003–1011.
19. Cancer Genome Atlas Network (2012) Comprehensive molecular characterization of human colon and rectal cancer. *Nature* 487(7407):330–337.
20. Bass AJ, et al. (2011) Genomic sequencing of colorectal adenocarcinomas identifies a recurrent VTI1A-TCF7L2 fusion. *Nat Genet* 43(10):964–968.
21. Starr TK, et al. (2009) A transposon-based genetic screen in mice identifies genes altered in colorectal cancer. *Science* 323(5922):1747–1750.
22. Barker N, et al. (2009) Crypt stem cells as the cells-of-origin of intestinal cancer. *Nature* 457(7229):608–611.
23. Zhu L, et al. (2009) Prominin 1 marks intestinal stem cells that are susceptible to neoplastic transformation. *Nature* 457(7229):603–607.
24. Sato T, et al. (2009) Single Lgr5 stem cells build crypt-villus structures in vitro without a mesenchymal niche. *Nature* 459(7244):262–265.
25. Case SS, et al. (1999) Stable transduction of quiescent CD34(+)CD38(-) human hematopoietic cells by HIV-1-based lentiviral vectors. *Proc Natl Acad Sci USA* 96(6):2988–2993.
26. Sato T, et al. (2011) Long-term expansion of epithelial organoids from human colon, adenoma, adenocarcinoma, and Barrett's epithelium. *Gastroenterology* 141(5):1762–1772.
27. Sato T, et al. (2011) Paneth cells constitute the niche for Lgr5 stem cells in intestinal crypts. *Nature* 469(7330):415–418.
28. Sansom OJ, et al. (2004) Loss of Apc in vivo immediately perturbs Wnt signaling, differentiation, and migration. *Genes Dev* 18(12):1385–1390.
29. Jho EH, et al. (2002) Wnt/beta-catenin/Tcf signaling induces the transcription of Axin2, a negative regulator of the signaling pathway. *Mol Cell Biol* 22(4):1172–1183.
30. Donehower LA, et al. (1992) Mice deficient for p53 are developmentally normal but susceptible to spontaneous tumours. *Nature* 356(6366):215–221.
31. Clarke AR, Cummings MC, Harrison DJ (1995) Interaction between murine germline mutations in p53 and APC predisposes to pancreatic neoplasia but not to increased intestinal malignancy. *Oncogene* 11(9):1913–1920.
32. Roberts RB, et al. (2002) Importance of epidermal growth factor receptor signaling in establishment of adenomas and maintenance of carcinomas during intestinal tumorigenesis. *Proc Natl Acad Sci USA* 99(3):1521–1526.
33. Beronja S, Livshits G, Williams S, Fuchs E (2010) Rapid functional dissection of genetic networks via tissue-specific transduction and RNAi in mouse embryos. *Nat Med* 16(7):821–827.
34. Tuveson DA, et al. (2004) Endogenous oncogenic K-ras(G12D) stimulates proliferation and widespread neoplastic and developmental defects. *Cancer Cell* 5(4):375–387.
35. Jackson EL, et al. (2001) Analysis of lung tumor initiation and progression using conditional expression of oncogenic K-ras. *Genes Dev* 15(24):3243–3248.
36. Ray KC, et al. (2011) Epithelial tissues have varying degrees of susceptibility to Kras (G12D)-initiated tumorigenesis in a mouse model. *PLoS ONE* 6(2):e16786.
37. Feng Y, et al. (2011) Mutant KRAS promotes hyperplasia and alters differentiation in the colon epithelium but does not expand the presumptive stem cell pool. *Gastroenterology* 141(3):1003–1013.
38. Raju J (2008) Azoxymethane-induced rat aberrant crypt foci: Relevance in studying chemoprevention of colon cancer. *World J Gastroenterol* 14(43):6632–6635.
39. Yamashita N, Minamoto T, Ochiai A, Onda M, Esumi H (1995) Frequent and characteristic K-ras activation and absence of p53 protein accumulation in aberrant crypt foci of the colon. *Gastroenterology* 108(2):434–440.
40. Pastrana E, Silva-Vargas V, Doetsch F (2011) Eyes wide open: A critical review of sphere-formation as an assay for stem cells. *Cell Stem Cell* 8(5):486–498.
41. Wang C, et al. (2012) Evaluation of CD44 and CD133 as cancer stem cell markers for colorectal cancer. *Oncol Rep* 28(4):1301–1308.
42. Yan KS, et al. (2012) The intestinal stem cell markers Bmi1 and Lgr5 identify two functionally distinct populations. *Proc Natl Acad Sci USA* 109(2):466–471.
43. Koo BK, et al. (2012) Controlled gene expression in primary Lgr5 organoid cultures. *Nat Methods* 9(1):81–83.
44. Shibata H, et al. (1997) Rapid colorectal adenoma formation initiated by conditional targeting of the Apc gene. *Science* 278(5335):120–123.
45. Hung KE, et al. (2010) Development of a mouse model for sporadic and metastatic colon tumors and its use in assessing drug treatment. *Proc Natl Acad Sci USA* 107(4):1565–1570.
46. Albuquerque C, et al. (2002) The 'just-right' signaling model: APC somatic mutations are selected based on a specific level of activation of the beta-catenin signaling cascade. *Hum Mol Genet* 11(13):1549–1560.
47. Fazeli A, et al. (1997) Effects of p53 mutations on apoptosis in mouse intestinal and human colonic adenomas. *Proc Natl Acad Sci USA* 94(19):10199–10204.
48. Schepers AG, et al. (2012) Lineage tracing reveals Lgr5+ stem cell activity in mouse intestinal adenomas. *Science* 337(6095):730–735.
49. Schwitalla S, et al. (2013) Intestinal tumorigenesis initiated by dedifferentiation and acquisition of stem-cell-like properties. *Cell* 152(1-2):25–38.
50. Powell AE, et al. (2012) The pan-ErbB negative regulator Lrig1 is an intestinal stem cell marker that functions as a tumor suppressor. *Cell* 149(1):146–158.
51. Montgomery RK, et al. (2011) Mouse telomerase reverse transcriptase (mTert) expression marks slowly cycling intestinal stem cells. *Proc Natl Acad Sci USA* 108(1):179–184.
52. Takeda N, et al. (2011) Interconversion between intestinal stem cell populations in distinct niches. *Science* 334(6061):1420–1424.

Nutrition and Cancer, 0(00), 1–11

ISSN: 0163-5581 print / 1532-7914 online
DOI: 10.1080/01635581.2014.847963

Routledge
Taylor & Francis Group

Green Tea Consumption and Breast Cancer Risk in Japanese Women: A Case-Control Study

Motoki Iwasaki
Epidemiology and Prevention Division, Research Center for Cancer Prevention and Screening, National Cancer Center, Tokyo, Japan

Junki Mizusawa
Clinical Trials Support Division, Center for Cancer Control and Information Services, National Cancer Center, Tokyo, Japan

Yoshio Kasuga
Department of Surgery, Nagano Matsushiro General Hospital, Nagano, Japan

Shiro Yokoyama and Hiroshi Onuma
Department of Breast and Thyroid Surgery, Nagano Red Cross Hospital, Nagano, Japan

Hideki Nishimura
Department of Surgery, Nagano Municipal Hospital, Nagano, Japan

Ritsu Kusama
Department of Surgery, Nagano Hokushin General Hospital, Nagano, Japan

Shoichiro Tsugane
Epidemiology and Prevention Division, Research Center for Cancer Prevention and Screening, National Cancer Center, Tokyo, Japan

Although many in vitro and animal studies have suggested a protective effect of green tea against breast cancer, only a few epidemiological studies have examined this association, and findings have been inconsistent. We examined the association between green tea consumption and breast cancer risk in consideration of the hormone receptor status of tumors and investigated whether the association was modified by dietary and genetic factors based on a hospital-based case-control study in Nagano, Japan. A total of 369 pairs completed a validated food frequency questionnaire and provided blood samples. Four single nucleotide polymorphisms (SNPs) were genotyped: *CYP19A1* (rs10046), *COMT* (rs4680), *MTHFR* C677T (rs1801133), and *MTHFR* A1298C (rs1801131). We found no inverse association between green tea consumption and breast cancer risk. Compared with women who drank less than 120 ml of green tea per day, the adjusted odds ratio for women who drank more than 600 ml was 1.27 (95% confidence interval = 0.75–2.14; *P* for trend = 0.20). We also found no inverse association for either tumor subtype. No substantial effect modification was observed for menopausal status, 4 SNPs, or dietary intake of folate or isoflavone. This study provides additional evidence that green tea consumption is not associated with a decreased risk.

Catechol-O-methyltrasferease

Submitted 10 May 2012; accepted in final form 4 June 2013.
Address correspondence to Motoki Iwasaki, Epidemiology and Prevention Division, Research Center for Cancer Prevention and Screening, National Cancer Center, 5-1-1 Tsukiji, Chuo-ku, Tokyo 104-0045, Japan. Phone: +81-3-3542-2511 (ext 3391) Fax: +81-3-3547-8578. E-mail: moiwasak@ ncc.go.jp

INTRODUCTION

Green tea is one of the most popular beverages in Japan and China, which have a lower risk of breast cancer than western countries (1). Because of its high levels of catechins, green tea has been hypothesized to have a protective effect against breast cancer (2). To date, 3 case-control and 5 cohort studies have investigated the association between green tea consumption and breast cancer risk, but findings have been inconsistent (3–10). A recent meta-analysis showed an inverse association for the case-control studies but no association for the cohort studies,

with odds ratios (OR) for the highest vs. lowest group of 0.70 [95% confidence interval (CI) = 0.61–0.79] for the former and 1.06 (95% CI = 0.93–1.20) for the latter (2). This difference between study types might be explained by the influence of recall and selection bias stemming from the case-control design; by differences in the type of tea and drinking methods (10); or by differences in the distribution of effect modifiers. As examples of the influence of effect modifiers, a case-control study in Asian American residents of Los Angeles County observed a risk-reducing effect primarily among subjects whose soy intake was low (3), whereas a nested case-control study in Singapore showed a protective effect among women with high-activity genotypes for *methylenetetrahydrofolate reductase* (*MTHFR*) and *thymidylate synthase* (*TYMS*) (8), particularly among those whose dietary folate intake was low.

Proposed mechanisms for green tea's decrease in the risk of breast cancer include strong antioxidant activity, inhibition of cell proliferation and angiogenesis, and induction of apoptosis (11). Green tea catechins have antiestrogenic properties, with green tea extracts inhibiting aromatase (12) and [(-)-epigallocatechin-3-gallate (EGCG)] inhibiting the binding of estrogen to its receptor (13). In cross-sectional studies, green tea consumption has been associated with a lower level of estrogen among premenopausal Japanese women (14) and postmenopausal Chinese women in Singapore (15). Given that the putative effect of green tea on the development of breast cancer might be mediated by estrogen exposure, we hypothesized that green tea consumption would be more closely associated with hormone receptor-positive than -negative breast cancer. However, only a few studies have investigated the association between green tea consumption and the risk of hormone receptor-defined subtype (10).

Here, using data from a hospital-based case-control study in Nagano, Japan, we investigated the association between green tea consumption and breast cancer risk in consideration of the hormone receptor status of tumors. We also examined whether the association was modified by dietary and genetic factors, which have been suggested as potential effect modifiers by previous reports (3,8,9,16).

MATERIALS AND METHODS

Study Subjects

This multicenter, hospital-based case-control study was conducted from May 2001 to September 2005 at 4 hospitals in Nagano Prefecture, Japan. Details of the study design and methods have been described elsewhere (17,18). Briefly, eligible case patients were a consecutive series of female patients aged 20–74 yr with newly diagnosed and histologically confirmed invasive breast cancer among hospitalized patients at 4 hospitals in Nagano Prefecture during the study period. Of the 412 eligible patients, 405 (98%) agreed to participate. Eligible control subjects were selected from medical checkup examinees in 2 of the hospitals who were confirmed to not have any cancer, with 1 control matched with each case by age (within 3 yr) and residential area. One control whose date of medical checkup was closest to the date of our examination of the index case was recruited from potential controls. Among potential controls, one examinee refused to participate and 2 refused to provide blood samples. We accordingly obtained written informed consent from 405 matched pairs. The study protocol was approved by the institutional review board of the National Cancer Center, Tokyo, Japan.

Data Collection

Participants were asked to complete a self-administered questionnaire, which contained questions on demographic characteristics, anthropometric factors, smoking habits, family history of cancer, physical activity, medical history, menstrual and reproductive history, and dietary habits. Information on estrogen receptor (ER) and progesterone receptor (PR) status was obtained from medical records. Hormone receptor status was determined by either enzyme-linked immunoassay or immunohistochemical assay. Hormone receptor positivity values were determined either as specified by the laboratory that performed the assay, or in accordance with the laboratory's written interpretation thereof, or both. Participants provided blood at the time they returned their self-administered questionnaire. Whole blood in 7 mL EDTA-2Na Vacutainer and serum samples were stored at −80°C until they are analyzed.

Exposure Assessment

The consumption of beverages during the previous year, including 2 items of green tea, namely *Sencha* (first or second flush of green tea, i.e., first seasonal picking)/*Bancha* (third or fourth flush of green tea, i.e., late seasonal picking) and *Houjicha* (roasted green tea, usually *Bancha*)/*Genmaicha* (blend of *bancha* and roasted brown rice); oolong tea; black tea; and coffee or canned coffee was assessed in terms of frequency and amount using the nine precoded categories of less than 1 cup per wk, 1–2 cups per wk, 3–4 cups per wk, 5–6 cups per wk, 1 cup per day, 2–3 cups per day, 4–6 cups per day, 7–9 cups per day, and 10 or more cups per day. The amount of *Sencha/Bancha* or *Houjicha/Genmaicha* consumed (ml per day) was computed by multiplying the frequency by the portion size for each beverage (120 ml per cup). Total green tea intake was defined as the sum of *Sencha/Bancha* and *Houjicha/Genmaicha* consumption.

Dietary habits were investigated using a 136-item semiquantitative food frequency questionnaire (FFQ) that was developed and validated in a Japanese population (19,20). In the FFQ, participants were questioned on how often they consumed the individual food items (frequency of consumption), as well as relative sizes compared to standard portions. Daily food intake was calculated by multiplying frequency by the standard portion and relative size for each food item in the FFQ. Daily intake of nutrients was calculated using the fifth revised and enlarged edition of the *Standard Tables of Food Composition in Japan* (21).

Genotyping

Genomic DNA samples were extracted from peripheral blood using Qiagen FlexiGene® DNA Kits (Qiagen K.K., Tokyo, Japan) according to the manufacturer's protocol. We selected 4 single-nucleotide polymorphisms (SNPs) in *aromatase* (*CYP19A1*), *catechol-O-methyltransferase* (*COMT*), and *MTHFR* (*CYP19A1* [rs10046], *COMT* [rs4680], *MTHFR* C677T [rs1801133], and *MTHFR* A1298C [rs1801131]) for the present study on the basis of suggestions that genotypes of *COMT* and *MTHFR* modify the association of green tea consumption and breast cancer (8,16). Genotyping of the 4 SNPs was performed by a commercial laboratory (Genetic Lab., Sapporo, Japan) using TaqMan SNP Genotyping Assays developed by Applied Biosystems (Foster City, CA).

Statistical Analysis

We excluded subjects who reported extremely low or high total energy intake (<500 or ≥4000 Kcal), had no information on green tea consumption or genotypes of the four SNPs, or had no DNA sample, leaving 369 pairs for use in the present analyses.

Baseline characteristics of cases and controls were compared by the Mantel-Haenszel test using matched-pair strata. Genotype frequencies were tested for deviation from the Hardy-Weinberg equilibrium by the chi-square test. We categorized subjects into 3 groups: 1–119 ml per day, 120–599 ml per day, and more than 600 ml per day based on total green tea consumption; and less than 1 cup per day, 1–3 cups per day, and 4 or more cups per day based on the frequency of *Sencha/Bancha* or *Houjicha/Genmaicha* consumption. Using a conditional logistic regression model, we calculated ORs and 95% CIs of breast cancer for green tea consumption. Stratified analyses by potential effect modifiers were performed using an unconditional logistic regression model. Associations between consumption and hormone receptor-defined breast cancer were assessed by an unconditional polytomous logistic regression model. The Wald test was used to test the null hypothesis that estimates were equal across hormone receptor-defined breast cancer subtypes. Linear trends for ORs were tested in the logistic regression model using the exposure categories as ordinal variables. Tests for interaction were performed based on the difference between 2 likelihood ratios of the models with and without the interaction terms between consumption and potential effect modifiers. In addition to matching factors, the following variables were adjusted as potential confounders: menopausal status (premenopausal women, postmenopausal women), number of births (0, 1, 2, 3, 4, 5+), family history of breast cancer (yes, no), smoking status (never, past, current smokers), moderate physical activity in the past 5 yr (no, less than 3 days/mo, 1–4 days/wk, more than 5 days/wk), vitamin supplement use (yes, no), oolong tea intake (less than 1 cup per wk, 1–6 cups per wk, 1 or more cups per day), black tea intake (less than 1 cup per wk, 1–6 cups per wk, 1 or more cups per day), coffee intake (less than 1 cup per wk, 1–6 cups per wk, 1 or more cups per day), and canned coffee intake (less than 1 cup per wk, 1–6 cups per wk, 1 or more cups per day). All reported P values are 2-sided, and significance level was set at $P < 0.05$. All statistical analyses were performed with SAS software version 9.2 (SAS Institute, Inc., Cary, NC).

RESULTS

Characteristics of case patients and control subjects are shown in Table 1. The proportion of premenopausal women, current smokers, and vitamin supplement users was higher in cases than in controls; and cases tended to have a family history of breast cancer and history of benign breast disease. Cases were less likely than controls to breastfeed and be physically active. Among 369 breast cancer cases, 138 (37.4%) cases were stage I and 190 cases (51.5%) were stage II based on the TNM classification of malignant tumors by the international union against cancer. Major histologic types were invasive ductal carcinoma (85.6%), invasive lobular carcinoma (4.1%), and mucinous carcinoma (3.8%). Genotype frequencies of each SNP were consistent with the Hardy-Weinberg equilibrium.

We found no inverse association between green tea consumption and the risk of breast cancer (Table 2). Compared with women who drank less than 120 ml of green tea per day, the adjusted OR for women who drank more than 600 ml was 1.27 (95% CI = 0.75–2.14; P for trend = 0.20). No substantial change was seen after further adjustment for other potential confounders, including education, age at menarche, age at menopause, age at first birth, history of breast feeding, body mass index, alcohol drinking, and vegetable and isoflavones intake (data not shown). We further categorized subjects into tertiles or quintiles based on distribution among the control group. However, no inverse association was observed regardless of categorization method (data not shown). Analyses based on the frequency of *Sencha/Bancha* or *Houjicha/Genmaicha* drinking also showed no inverse association: compared with women who drank less than 1 cup of *Sencha/Bancha* or *Houjicha/Genmaicha* per day, adjusted ORs for women who drank 4 or more cups were 1.15 (95% CI = 0.71–1.86; P for trend = 0.56) for *Sencha/Bancha* and 1.42 (95% CI = 0.74–2.69; P for trend = 0.12) for *Houjicha/Genmaicha* (data not shown in Table 2).

Information on the combined ER and PR status of tumors was available for 366 (99%) of 369 patients. The following subtypes were used for modeling in an unconditional polytomous logistic regression model: positive for both receptors (ER+/PR+), ER-positive and PR-negative (ER+/PR-), and negative for both receptors (ER-/PR-). ER-negative and PR-positive (ER-/PR+) cases were excluded owing to their small number ($n = 12$). We found no inverse association between green tea consumption and risk regardless of subtype (Table 2). Instead, women who drank more than 600 ml per day tended to be at higher risk of ER-PR- tumors, albeit without statistical significance.